Technical Support Document for the Clear Skies Act 2003 Air Quality Modeling Analyses

U.S. Environmental Protection Agency
Office of Air Quality Planning and Standards
Emissions Analysis and Monitoring Division
Research Triangle Park, NC 27711

October 2003

Table of Contents

I. Introduction

This document describes the procedures and results of the air quality modeling analyses used to quantify the impacts and benefits of the Clear Skies Act (CSA) of 2003. The air quality modeling was conducted to support several components of the legislation including:

(a) an assessment of the costs and benefits associated with the Act, and
(c) an assessment of the expected impact of the Act on ozone and $PM_{2.5}$ levels.

The air quality model applications include episodic regional scale ozone modeling for the Eastern U.S. and annual particulate matter (PM), visibility, and deposition modeling on a continental scale covering the 48 contiguous States. 1996 Base Year simulations were made to examine the ability of the modeling systems to replicate observed concentrations of these pollutants. This was followed by simulations using a 2001 "proxy" emissions inventory. The 2001 inventory was created for the purpose of aligning the current year ozone and $PM_{2.5}$ design values (1999-2001) to the emissions inventory year.

The 2001 modeling was followed by simulations for future-year base case scenarios of 2010 and 2020. The future base case scenarios included emissions resulting from growth and known emissions controls from Federal and State rules and legislation. The results of the future base case model runs were used to establish a base to compare against the Clear Skies controls. Additional control case simulations were performed for 2010 and 2020 to quantify the impacts of the Clear Skies Act controls on air quality. The outputs of the base and control case model runs were also used to calculate portions of the monetized benefits as part of the cost-benefits analysis.

The remainder of this report includes a description of the ozone and PM/visibility/deposition modeling systems, the time periods modeled, the Base Year (1996) model performance evaluations, and the results of the future Base Case and Control Case model simulations.

II. Emissions Inventory Estimates

In order to complete the requisite ozone and PM modeling, it was necessary to first develop a national mass emissions inventory. This mass emissions inventory was then used as the basis for developing input files for the air quality modeling. The development and details of these inventories for each of the scenarios (i.e., 1996 base year, 2001 base case, 2010 base case, 2010 control case, 2020 base case, and 2020 control case) are described elsewhere (EPA, 2003a) and (EPA, 2003b).

The mass inventories were prepared at the county-level for on-highway mobile, stationary area sources, and nonroad sources. Emissions for electric generating units (EGUs)

and large industrial sources (non-EGUs) were prepared as individual point sources. These inventories contain annual and typical summer season day emissions for the following pollutants: oxides of nitrogen (NO_X), volatile organic compounds (VOC), carbon monoxide (CO), sulfur dioxide (SO_2), primary particulate matter with an aerodynamic diameter less than or equal to 10 micrometers and 2.5 micrometers (PM_{10} and $PM_{2.5}$), ammonia (NH_3), and mercury (Hg). The 2010 and 2020 non-EGU and area source base case inventories were prepared by applying growth and control assumptions to the 1996 base year inventory. The 2010 and 2020 mobile and nonroad base case inventories were developed by applying the MOBILE5b[1] and NONROAD2002 models respectively. The EGU base case emissions were developed from the IPM model (EPA, 2003) . The 2010 and 2020 control case inventories are the same as the 2010 and 2020 base case inventories for all sectors except for EGU emissions. The Clear Skies control case EGU emissions are supplied by IPM.

The annual and summer day mass emissions inventories for each scenario were processed using the SMOKE (Houyoux, 2000) to create the appropriate emissions inputs for REMSAD and CAMx model runs, respectively. The emissions processing produced hourly, gridded, speciated emissions. For PM modeling the annual emissions for stationary area, point, and nonroad sources were processed to generate separate sets of emissions representing typical weekday, Saturday, and Sunday emissions for each season. For ozone modeling the summer day emissions were processed to generate typical summer weekday, Saturday, and Sunday emissions. On-highway emissions were obtained in model-ready form from the Heavy-Duty Diesel Rule modeling exercise. Hourly biogenic emissions were calculated using the Biogenic Emissions Inventory System (BEIS3.09) model. Biogenic emissions were not altered for any of the scenarios modeled. Appendix A contains State by State emissions summaries of total emissions from all sectors as well as annual total EGU emissions for each of the modeling scenarios. More detailed emissions summaries (for all source sectors) can be found at: ftp://ftp.epa.gov/modelingcenter/Clear_skies/CSA2003/Emissions/Summaries/CSA-2003-Emissions-Summaries.zip

III. Episodic Ozone Modeling

Air quality modeling analyses for ozone were conducted with the Comprehensive Air Quality Model with Extensions (CAMx). CAMx is non-proprietary computer modeling tool that can be used to evaluate the impacts of proposed emissions reductions on future air quality levels. For more information on the CAMx model, please see the model user's guide (Environ, 2002)[2]. Version 3.10 of the CAMx model was employed for these analyses.

---

[1] The mobile source inventories were prepared using MOBILE5b with adjustment factors to simulate MOBILE6 emissions. These are the same mobile source emissions that were used in the Nonroad rule proposal and the Heavy Duty Engine and Tier 2 rules.

[2] http://www.camx.com/pdf/CAMx3.UsersGuide.020410.pdf

The modeling analyses were completed for an Eastern U.S. domain as shown in Figure III-1. The domain has nested horizontal grids of 36 and 12 km. The model was applied and evaluated over three episodes that occurred during the summer of 1995 base year. Subsequently, episodic ozone model runs were made for the 2001 base year scenario and the 2010 and 2020 base and control case scenarios for all episodes.

The model output from the 1996 base year scenario was used to evaluate the performance of the model. The model outputs from the 2001 base year and 2010 and 2020 base and control cases, combined with current air quality data, were used to project ozone design values to the future years (2010 and 2020). The costs, benefits, and expected impacts of the proposed controls were determined by comparing the model results in the future year control runs against the baseline simulations of the same year.

A. Model Configuration

1. Episodic Meteorology and Ambient Air Quality

There are several considerations involved in selecting episodes for an ozone modeling analysis (EPA, 1999a). In general, the goal should be to model several differing sets of meteorological conditions leading to ambient ozone levels similar to an area's design value. Warm temperatures, light winds, cloud-free skies, and stable boundary layers are some of the typical characteristics of ozone episodes. On a synoptic scale, these conditions usually result from a combination of high pressure aloft (e.g., at the 500 millibar pressure level) and at the surface. Of course at a smaller scale, the conditions that lead to local ozone exceedances can vary from location to location based on factors such as wind direction, sea/lake breezes, etc. The meteorological and resultant ozone patterns for the three separate modeling episodes used in this analysis are listed in Table III-1 and are discussed in more detail in previous technical support documents for the Tier-2/Low Sulfur rule (EPA, 1999b) and the Heavy-Duty Engine rule (EPA, 2000). These previous discussions conclude that the selected episodes contain measured ozone concentrations that are representative of design values over most of the eastern U.S. The first three days of each period are considered ramp-up days and the results from these days were not used in the analyses. In all, 30 episode days were modeled.

Table III-1. Dates of CAMx Modeling Episodes.

	Eastern U.S. Modeling
Episode 1	June 12-24, 1995
Episode 2	July 5-15, 1995
Episode 3	August 7-21, 1995

2. Domain and Grid Configuration

As with episode selection, there are also several considerations involved in selecting the domain and grid configuration to be used in the ozone modeling analysis. The modeling domain should encompass the area of intended analysis with an additional buffer of grid cells to minimize the effects of uncertain boundary condition inputs. When possible, grid resolution should be equivalent to the resolution of the primary model inputs (emissions, winds, etc.) and equivalent to the scale of the air quality issue being addressed. The CAMx modeling was performed for the coarse and fine grid domains as defined below.

Table III-2. Details of the CAMx Modeling Domains.

	Eastern US Domain	
	Coarse Grid	**Fine Grid**
Map Projection	latitude/longitude	latitude/longitude
Grid Resolution	1/2˚ longitude, 1/3˚ latitude (~ 36 km)	1/6˚ longitude, 1/9˚ latitude (~ 12 km)
East/West extent	-99 W to -67 W	-92 W to -69.5 W
North/South extent	26 N to 47 N	32 N to 44 N
Vertical extent	Surface to 4 km	Surface to 4 km
Dimensions	64 by 63 by 9	137 by 110 by 9

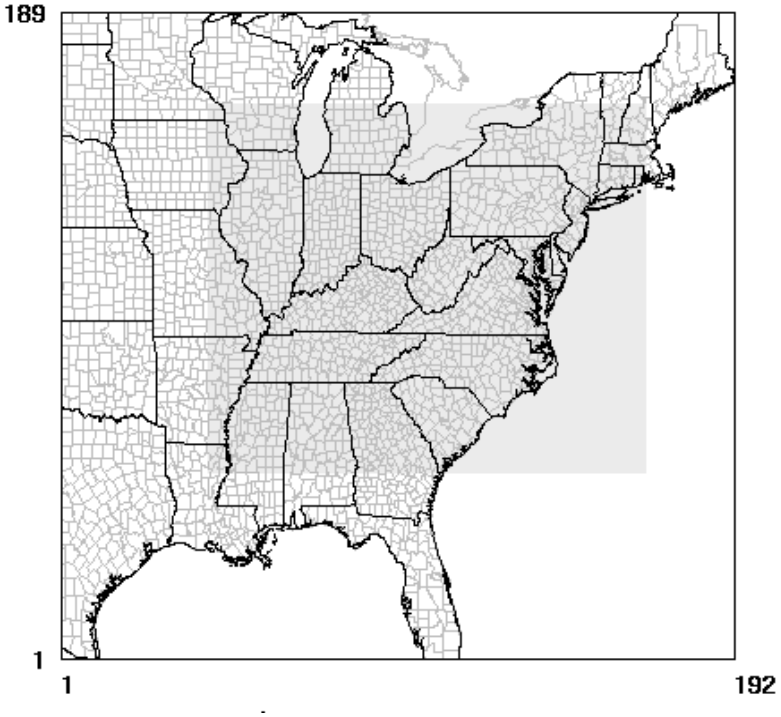

Figure III-1. Map of the Eastern U.S. modeling domain. The outer box denotes the entire modeling domain (36 km) and the inner box shaded indicates the fine grid location (12 km).

3. Meteorological and Other Model Inputs

The air quality model requires certain meteorological inputs that, in part, govern the formation, transport, and destruction of pollutant material. In particular, the CAMx model used in these analyses requires seven meteorological input files: wind (u- and v-vector wind components), temperature, water vapor mixing ratio, atmospheric air pressure, cloud cover, rainfall, and vertical diffusion coefficient. Fine grid values of wind, pressure, and vertical diffusivity are used; the other fine grid meteorological inputs are interpolated from the coarse grid files.

Eastern U.S. Domain: The gridded meteorological data for the three historical 1995 episodes were developed by the New York Department of Environment and Conservation using the Regional Atmospheric Modeling System (RAMS), version 3b. RAMS (Pielke *et. al.*, 1992) is a numerical meteorological model that solves the full set of physical and thermodynamic equations which govern atmospheric motions. The output data from RAMS, which was run in a polar stereographic projection and a sigma-p coordinate system, was then mapped to the CAMx grid.

Two separate meteorological CAMx inputs, cloud fractions and rainfall rates, were developed based on observed data.

RAMS was run in a nested-grid mode with three levels of resolution: 108 km, 36 km, and 12 km with 28-34[3] vertical layers. The top of the surface layer was 16.7 m in the 36 and 12km grids. The two finer grids were at least as large as their CAMx counterparts. In order to keep the model results in line with reality, the simulated fields were nudged to an European Center for Medium-Range Weather Forecasting analysis field every six hours. This assimilation data set was bolstered by every four-hourly special soundings regularly collected as part of the North American Research Strategy on Tropospheric Ozone field study in the northeast U.S.

A limited model performance evaluation (Sistla, 1999) was completed for a portion of the 1995 meteorological modeling (July 12-15). Observed data not used in the assimilation procedure were compared against modeled data at the surface and aloft. In general, there were no widespread biases in temperatures and winds. Furthermore, the meteorological fields were compared before and after being processed into CAMx inputs. It was concluded that this preprocessing did not distort the meteorological fields.

Other Model Inputs: In addition to the meteorological data, the photochemical grid model requires several other types of data. In general, most of these miscellaneous model files were taken from existing regional modeling applications. Clean conditions were used to initialize the model and as lateral and top boundary conditions as in previous regional modeling applications. The model also requires information regarding land use type and surface albedo for all layer 1 grid cells in the domain. Existing regional data obtained from OTAG were used for these non-day-specific files. Photolysis rates were developed using the JCALC preprocessor (SAI, 1996). Turbidity values were set equal to a constant thought to be representative of regional conditions.

[3] The inner nests were modeled with 34 layers while the outer 108 km domain was modeled with 28 layers.

B. Model Performance Evaluation

The goal of the Base Year modeling was to reproduce the atmospheric processes resulting in high ozone concentrations over the eastern United States during the three 1995 episodes selected for modeling. Note that the Base Year of the emissions was 1996 while the eastern U.S. episodes are for 1995. The effects on model performance of using 1996 Base Year emissions for the 1995 episodes are not known, but are not expected to be major.

An operational model performance evaluation for surface ozone for the three episodes was performed in order to estimate the ability of the modeling system to replicate base year ozone concentrations. This evaluation is comprised principally of statistical assessments of model versus observed pairs. The robustness of an operational evaluation is directly proportional to the amount and quality of the ambient data available for comparison.

1. Statistical Definitions

Below are the definitions of those statistics used for the evaluation. The format of all the statistics is such that negative values indicate model ozone predictions that were less than their observed counterparts. Positively-valued statistics indicate model overestimation of surface ozone. Statistics were not generated for the first three days of an episode to avoid the initialization period. The operational statistics were principally generated on a regional basis in accordance with the primary purpose of the modeling which is to assess the need for, and impacts of, a national emissions control program. However, a local assessment of model performance was also completed to ensure that the model did not significantly overestimate the need for controls in individual areas. The statistics were calculated for (a) the entire domain, (b) four quadrants (i.e., Midwest, Northeast, Southeast, Southwest), and (c) 47 local areas. The statistics calculated for each of these sets of areas are described below.

Domainwide unpaired peak prediction accuracy: This metric simply compares the peak concentration modeled anywhere in the selected area against the peak ambient concentration anywhere in the same area. The difference of the peaks (model - observed) is then normalized by the peak observed concentration.

Peak prediction accuracy: This metric averages the paired peak prediction accuracy calculated for each monitor in the subregion. It characterizes the ability of the model to replicate peak (afternoon) ozone over a subregion. The daily peak model versus daily peak observed residuals are paired in space but not by hour.

Mean normalized bias: This performance statistic averages the normalized (by observation) difference (model - observed) over all pairs in which the observed values were greater than 60 ppb. A value of zero would indicate that the model over predictions and model under predictions exactly cancel each other out.

Mean normalized gross error: The last metric used to assess the performance is similar to the

above statistic, except in this case it is the absolute value of the residual which is normalized by the observation, and then averaged over all sites. A zero gross error value would indicate that all model concentrations (in which their observed counterpart was greater than 60 ppb) exactly matched the ambient values.

2. Domainwide Model Performance

As with previous regional photochemical modeling studies, the degree that model predictions replicate observed concentrations varies by day and location over the large eastern U.S. modeling domain. From a qualitative standpoint, there appears to be considerable similarity on most days between the observed and simulated ozone patterns. Additionally, where possible to discern, the model appears to follow the day-to-day variations in synoptic-scale ozone fairly closely. More quantitative comparisons of the model predictions and ambient data are provided below.

When all hourly observed ozone values (greater than 60 ppb) are compared to their modeled counterparts for the thirty episode modeling days for the eastern U.S., the mean normalized bias is -1.1 percent and the mean normalized gross error is 20.5 percent As shown in Table III-3, the model generally underestimates observed ozone values for the June and July episodes, but predicts higher than observed amounts for the August episode.

Table III-3. Performance statistics for hourly ozone in the Eastern U.S. CAMx simulations.

	Average Accuracy of the Peak	Mean Normalized Bias	Mean Normalized Gross Error
June 1995	-7.3	-8.8	19.6
July 1995	-3.3	-5.0	19.1
August 1995	9.6	8.6	23.3

Depending on the episode and region, the normalized biases can range from an underestimation of 18 percent to an overestimation of 16 percent. Gross errors tend to average between 17 and 25 percent. As shown in Table III-4, when the model domain is subdivided into four quadrants, it is found that most of the underestimations in the June and July episodes are driven by the Northeast and Midwest quadrants (i.e., the two northern ones). Conversely, most of the overestimated ozone in the August episode is due to the Midwest, Southeast and Southwest quadrants. Hourly ozone is consistently underestimated in the Northeast quadrant. The model does slightly better in replicating the peak values for each monitoring site than it does at replicating the mean values, especially in the Northeast where the underpredictions are not as large for the highest ozone observations.

Table III-4. Regional/Episodic performance statistics for Clear Skies hourly ozone predictions.

	Average Accuracy of the Peak			Mean Normalized Bias			Mean Normalized Gross Error		
	June	*July*	*August*	*June*	*July*	*August*	*June*	*July*	*August*
Whole Grid	-7.3	-3.3	9.6	-8.8	-5.0	8.6	19.6	19.1	23.3
Northeast	-14.7	-5.0	-4.3	-18.4	-7.2	-6.0	24.7	19.1	22.6
Midwest	-7.3	-6.2	15.5	-8.7	-7.2	15.5	18.0	19.4	23.7
Southeast	-2.9	1.9	15.1	-3.0	1.3	14.7	17.4	19.1	24.1
Southwest	-0.9	1.3	7.0	0.7	3.1	10.3	19.0	20.0	22.6

At present, there are no generally accepted set of numerical criteria by which one can judge the adequacy of model performance for regional applications. In view of this, EPA determined the acceptability of modeling for Clear Skies by comparison against the performance results of regional models from previous analyses. For instance, the Nonroad rule Heavy Duty Engine (HDE) simulations were determined to be appropriate for use based on comparisons to previously accepted modeling analyses (e.g., OTAG and Tier-2). As shown in Table III-5, model performance in the base year Clear Skies simulations is generally similar or better than other regional ozone modeling efforts. In particular, the gross error metric is almost universally improved in the more recent Clear Skies modeling. In general, the Clear Skies/CAMx modeling results are approximately 3-6 ppb higher on average than what was generated in the HDE/UAM-V modeling. In some previous regional modeling applications, there had been a tendency in some regions for the model to underestimate ozone in the early parts of an episode and then overestimate ozone at the end of an episode. However, in general, there does not appear to be any such bias trend in the Clear Skies base year modeling.

Table III-5. Regional/Episodic performance statistics for HDE hourly ozone predictions. Bold numbers indicate HDE statistics that have improved in the Clear Skies simulations (see Table III-4).

	Average Accuracy of the Peak			Mean Normalized Bias			Mean Normalized Gross Error		
	June	*July*	*August*	*June*	*July*	*August*	*June*	*July*	*August*
Whole Grid	**-10.5**	**-5.8**	7.7	**-13.2**	**-9.6**	5.0	**22.3**	**22.3**	**23.6**
Northeast	**-15.1**	**-6.6**	**-5.2**	**-20.3**	**-12.1**	**-8.8**	**27.0**	**21.2**	**24.2**
Midwest	**-13.1**	**-11.1**	11.4	**-15.4**	**-14.2**	9.6	**21.6**	**23.6**	22.1
Southeast	**-5.4**	0.6	14.7	**-7.2**	**-2.8**	12.1	**18.4**	**21.0**	**24.6**
Southwest	0.2	**3.9**	**8.8**	**1.0**	**4.9**	**10.5**	**21.6**	**23.4**	**26.5**

Table III-6 presents the results from the eight-8-hour ozone evaluation. In general, the gross error is noticeably less for the eight-hour ambient versus observed ozone comparisons. However, model estimates during the August episode clearly over predict the observed values in regions outside the Northeast.

Table III-6. Regional/Episodic performance statistics for Clear Skies 8-hour ozone predictions.

	Average Accuracy of the Peak			**Mean Normalized Bias**			**Mean Normalized Gross Error**		
	June	*July*	*August*	*June*	*July*	*August*	*June*	*July*	*August*
Whole Grid	-3.9	0.9	13.9	-5.7	-2.1	11.0	17.5	16.4	22.6
Northeast	-13.5	-2.4	-1.6	-15.4	-4.9	-3.8	21.3	14.6	20.8
Midwest	-4.0	-0.9	20.6	-5.8	-4.4	17.6	16.0	16.7	23.7
Southeast	1.3	5.3	20.5	0.9	4.0	18.4	16.4	17.5	24.1
Southwest	5.0	8.2	16.2	3.9	3.6	12.4	17.8	18.1	21.1

3. Local-scale Model Performance

The CAMx modeling results were also evaluated at a "local" level. The purpose of this analysis was to ensure that areas determined to need the nonroad engine emissions reductions based on projected exceedances of the ozone standard were not unduly influenced by local overestimation of ozone in the model Base Year. For this analysis, the modeling domain was broken up into 51 local subregions as shown in Figure III-3. The primary statistics for each of the 51 subregions is shown in Table III-7.

As noted above, there is no set of established statistical benchmarks to determine the adequacy of a regional modeling operation evaluation. However, the performance statistics for the eastern U.S. modeling were compared to the recommended performance ranges for urban attainment modeling (EPA, 1991). The results indicate that model performance for the June episode was within the recommended ranges for 69% of the local areas examined. For the July and August episodes, the percent of local areas with performance within the recommended ranges was 80% and 61%, respectively. This is an improvement from the HDE model performance where the numbers were 57%, 45%, and 55% for the June, July, and August episodes, respectively.

Local scale model performance is poorest in the southeastern U.S. in the August episode where over predictions occurred. In fact, areas along the Gulf Coast (New Orleans, Beaumont/Port Arthur, Baton Rouge, etc.) tend to be universally overestimated. This is likely due to the model tendency to generate large amounts of ozone along coastal areas where low stability and high emissions densities can coexist.

With the exception of the July episode, the model tends to underestimate observed ozone by approximately 15% in the local areas of the Northeast (e.g., New York City, Philadelphia, Boston). The local 8-hour metrics (not shown) generally do not greatly differ from their hourly counterparts. There is a slight tendency toward greater overprediction of the 8-hour values.

Table III-7. Local performance statistics for Clear Skies hourly ozone predictions.

	Average Accuracy of the Peak			**Mean Normalized Bias**			**Mean Normalized Gross Error**		
	June	*July*	*August*	*June*	*July*	*August*	*June*	*July*	*August*
Dallas	-9.6	-12.3	2.2	-10.6	-11.5	3.2	16.6	18.7	15.7
Houston/Galveston	-3.0	-5.1	0.3	-3.5	-3.9	2.2	20.8	19.0	25.7
Beaumont/Port Arthur	14.0	16.7	8.8	16.0	19.3	12.9	20.4	24.5	24.6
Baton Rouge	15.6	24.7	31.4	22.6	26.6	37.4	26.1	31.0	40.5
New Orleans	15.6	29.1	42.1	15.9	28.9	48.9	21.9	32.0	50.2
St. Louis	-0.5	-4.0	8.4	-0.6	0.6	10.5	17.0	18.4	18.2
Memphis	-7.7	-4.9	13.7	-5.9	-0.3	13.6	15.5	19.3	22.0
Alabama	5.2	-1.7	16.0	6.5	6.7	23.1	14.4	16.6	25.2
Atlanta	-3.1	5.4	19.0	-3.4	6.8	26.1	16.7	20.1	31.0
Nashville	-2.9	7.8	31.5	-2.4	9.1	36.1	18.1	24.7	37.4
Eastern TN	-14.2	-16.0	-2.7	-21.0	-17.1	-5.9	22.7	20.7	18.3
Charlotte	8.3	-2.1	6.0	5.8	4.1	14.5	13.0	16.3	18.2
Greensboro	-1.7	-1.1	17.2	-4.2	1.2	18.2	14.1	15.3	21.7
Raleigh-Durham	-11.8	1.3	-2.3	-10.7	4.2	-1.9	14.6	13.9	16.9
Evansville/Owensboro	1.2	-0.9	28.3	4.5	5.4	32.8	15.1	21.2	33.9
Indianapolis	-8.3	-13.5	15.9	-3.6	-14.4	18.0	13.1	19.3	19.7
Louisville	2.8	4.2	36.6	4.8	6.1	42.1	14.7	17.9	42.5
Cincinnati/Dayton	-4.7	-8.5	29.0	0.1	-5.6	32.7	12.8	19.1	33.5
Columbus	-8.5	-14.5	9.2	-6.2	-11.0	14.2	14.6	17.3	18.7
West Virginia	-8.8	-5.7	12.7	-7.5	-3.2	13.7	15.7	16.6	24.5
Chicago	-9.9	-4.3	10.4	-17.1	-11.1	3.5	24.5	23.5	22.3
Milwaukee	-14.8	-12.9	21.5	-16.5	-16.9	12.3	19.1	23.3	18.2
Muskegon/Grand Rapids	-10.8	-12.3	3.1	-11.6	-12.9	1.7	17.7	20.4	16.4
Gary/South Bend	-13.0	-10.0	11.8	-15.0	-14.5	9.3	19.2	24.4	20.7
Detroit	-17.2	-5.8	3.9	-20.1	-13.2	-3.2	25.1	22.5	23.4

Pittsburgh	-10.0	-3.2	9.2	-9.2	-2.1	7.9	23.1	16.1	20.4
Central PA	-6.0	-7.6	1.0	-8.5	-6.0	1.1	21.9	15.5	18.6
Norfolk	-9.0	0.0	8.3	-13.4	-5.6	5.7	19.1	18.6	24.7
Richmond	-1.2	4.8	2.6	-1.3	10.7	4.5	8.4	18.3	20.3
Baltimore/Washington	-4.7	-3.1	1.7	-6.8	-5.2	0.7	18.6	15.6	23.4
Delaware	-6.1	-5.2	2.3	-6.3	-0.2	7.5	12.9	11.6	16.2
Philadelphia	-14.1	-1.8	-8.7	-22.0	-10.5	-13.9	26.4	19.5	28.9
New York City	-16.2	-3.9	-12.2	-24.6	-14.1	-17.9	31.3	22.5	29.8
Hartford	-16.9	-5.0	-9.9	-18.5	-4.0	-7.7	23.6	18.2	20.1
Boston	-13.7	-4.7	-15.6	-19.6	-9.2	-19.6	25.9	20.9	26.5
Maine	-20.4	-4.7	-6.9	-25.0	-9.4	-6.9	25.3	19.0	15.5
Longview/Shreveport	-2.1	11.3	7.7	0.8	11.1	11.4	16.2	16.5	17.9
Kansas City	-8.5	-7.8	-4.3	-7.9	-1.5	-8.3	15.7	13.0	12.4
Western NY	-23.1	-20.6	-9.0	-25.6	-20.5	-12.1	28.1	23.8	19.0
Northeast OH	-4.0	-6.5	6.9	-6.6	-6.8	7.7	20.4	15.5	16.5
South Carolina	-2.5	1.3	11.4	-3.4	1.5	15.7	12.5	17.7	19.4
Gulf Coast	0.5	23.1	29.3	4.5	30.0	33.7	15.4	31.6	34.9
FL West Coast	-6.4	22.8	41.2	-7.3	11.9	42.8	11.3	22.7	43.7
FL East Coast	-15.9	16.2	23.3	-16.8	16.6	26.3	18.0	18.4	29.4
Jackson	0.6	10.9	21.0	1.8	10.0	24.0	16.0	16.0	24.9
Central MI	-6.9	-10.4	12.0	-9.6	-14.8	6.6	18.1	18.7	17.5
Macon/Columbus	-9.5	-11.1	21.6	-8.8	-5.7	26.4	10.9	13.0	26.9
Austin/San Antonio	-14.1	-19.6	-1.9	-11.0	-15.5	4.1	14.1	17.2	12.4
Oklahoma City/Tulsa	-12.3	-5.6	-5.2	-12.9	-3.2	-2.8	17.2	14.6	12.6
Ft. Wayne/Lima	-9.1	-13.1	3.9	-8.3	-14.1	5.1	16.0	18.2	10.6
Bangor/Hancock Co.	-17.8	-6.9	-17.7	-24.4	-8.5	-19.9	25.2	15.3	21.0

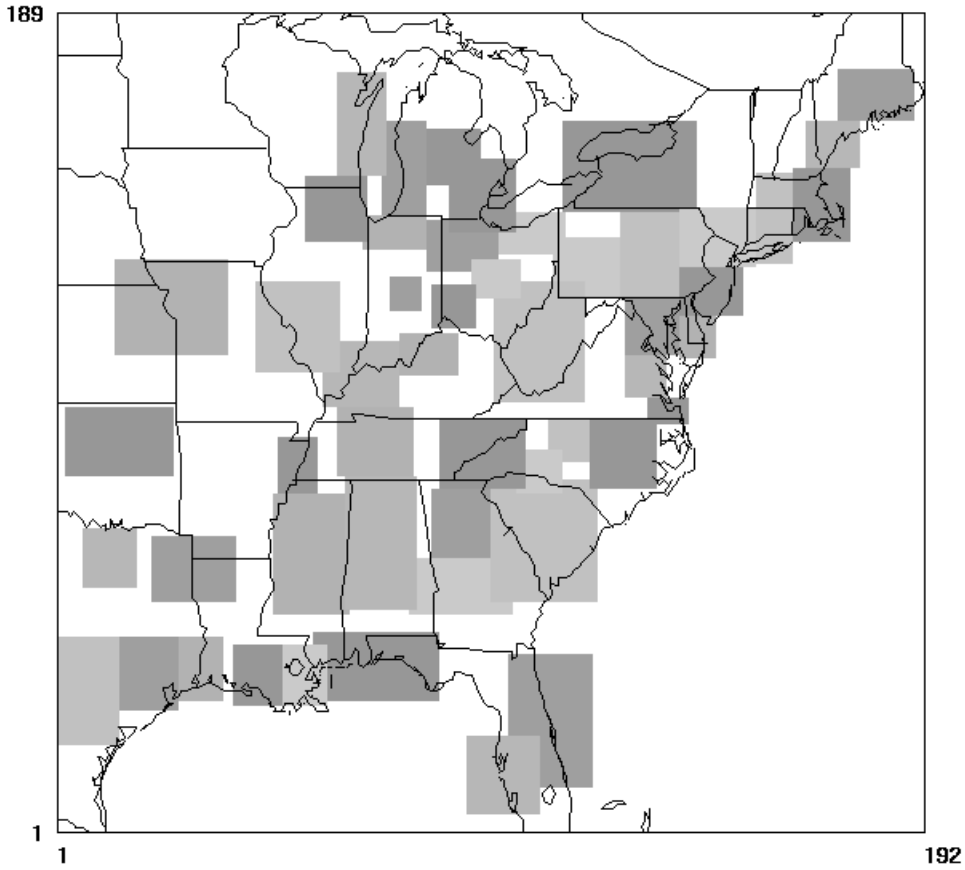

Figure III-3. Map of the 51 local-scale evaluation zones.

C. Ozone Modeling Results

The Clear Skies CAMx modeling output was analyzed to examine the air quality impacts of the legislation. The procedures and results of the analysis is described below.

1. Projected Future Ozone Design Values

a.) East

The CAMx simulations were performed for Base Cases in 1996, 2001, 2010, and 2020 considering growth and expected emissions controls that will affect future air quality. The effects of the Clear Skies Act emissions reductions (i.e., Control Cases) were modeled for the two future years (2010 and 2020). As a means of assessing the future levels of air quality with regard to the ozone NAAQS, future-year estimates of ozone design values were calculated using relative reduction factors (RRFs) applied to 1999-2001 ozone design values (EPA, 2003b). The procedures for determining the RRFs are similar to those in EPA's draft guidance for modeling for an 8-hour ozone standard (EPA, 1999a). Hourly model predictions were processed to

determine daily maximum 8-hour concentrations for each grid cell for each non-ramp-up day modeled. The RRF for a monitoring site was determined by first calculating the multi-day mean of the 8-hour daily maximum predictions in the nine grid cells surrounding the site using only those predictions greater than or equal to 70 ppb, as recommended in the guidance. This calculation was performed for the base year 2001 scenario and each of the future-year scenarios. The RRF for a site is the ratio of the mean prediction in the future-year scenario to the mean prediction in the base year scenario. RRFs were calculated on a site-by-site basis. The future-year design value projections were then calculated by county, based on the highest resultant design values for a site within that county from the RRF application. The current 8-hour county maximum ozone design values and future year base and control attainment status is provided in Appendix B. County populations are also included in this appendix.

b.) West

Western US ozone episodes were not modeled as part of the Clear Skies analysis due to the fact that all of predicted future year ozone nonattainment areas in the West are in California[4]. Clear Skies is predicted to reduce NO_X emissions in California by less than 0.2% in both 2010 and 2020 (~1300 tons per year). Therefore, it was assumed that Clear Skies would not affect the attainment status of any counties in California. But estimated future year nonattainment county counts for the West were still needed to portray the estimated nationwide 8-hour ozone nonattainment problem. The modeling results from the recently completed Nonroad Land Based Diesel Engine (NLDE) proposed rulemaking were used to develop base year 2010 and 2020 nonattainment county estimates for the West (EPA, 2003c). Western episodic ozone modeling was completed as part of the NLDE modeling. The future year model runs were completed for 2020 and 2030. For the Clear Skies analysis, the 2020 Nonroad modeling Western county counts were used directly. The 2010 Clear Skies estimates were derived by linearly interpolating the 2020 Nonroad values and the 1999-2001 ambient design values.

2. Ozone Nonattainment Summary

As shown in Table III-8, the modeling projects that 59 counties across the country with a population of 45.4 million people will have design values greater than the 8-hour NAAQS in 2010 without Clear Skies controls. By 2020 that number is expected to fall to 30 counties with a population of 39.5 million people as a result of projected emissions reductions from existing control programs.

Clear Skies emissions reductions are predicted to bring 5 counties into attainment in 2010 and cause 2 counties (Mecklenburg county NC and Henry county GA) to go out of attainment[5] in

[4]The only non-California county in the West that is currently not attaining the 8-hour standard is Maricopa county, AZ with a current (1999-2001) design value of 85 ppb. Through interpolation methods described above, the predicted 2010 design value for Maricopa county is 82 ppb. Therefore, all of the predicted 2010 and 2020 ozone nonattainment counties in the West are in California.

[5]It might seem unusual that there is an apparent predicted increase in ozone as a result of Clear Skies controls in several counties. When low level NO_X emissions are reduced, ozone can increase in

2010. The net reduction of 3 counties leaves 56 counties with a population of 44.5 million people nonattainment for the 8-hour ozone standard in 2010 after Clear Skies controls. In 2020 Clear Skies is expected to bring 3 counties into attainment. That leaves 27 counties with a population of 33.5 million people nonattainment for the 8-hour ozone standard in 2020 after Clear Skies controls. Appendix C contains maps of the base year and projected year 8-hour ozone nonattainment counties.

Table III-8. Lists of counties projected to violate the 8-hour NAAQS in 2010 and 2020 for the Base Case and Clear Skies Control Case.

2010 Base	2010 Control	2020 Base	2020 Control
California, Orange	California, Orange	California, Orange	California, Orange
California, Kings	California, Kings	California, Ventura	California, Ventura
California, Sacramento	California, Sacramento	California, Los Angeles	California, Los Angeles
California, Merced	California, Merced	California, Fresno	California, Fresno
California, Ventura	California, Ventura	California, Kern	California, Kern
California, El Dorado	California, El Dorado	California, Riverside	California, Riverside
California, Tulare	California, Tulare	California, San Bernardino	California, San Bernardino
California, Los Angeles	California, Los Angeles	Connecticut, Fairfield	Connecticut, Fairfield
California, Fresno	California, Fresno	Connecticut, New Haven	Connecticut, New Haven
California, Kern	California, Kern	Connecticut, Middlesex	Connecticut, Middlesex
California, Riverside	California, Riverside	Illinois, Cook	Michigan, Macomb
California, San Bernardino	California, San Bernardino	Indiana, Lake	Michigan, Wayne
Connecticut, Fairfield	Connecticut, Fairfield	Maryland, Harford	New Jersey, Hudson
Connecticut, New Haven	Connecticut, New Haven	Michigan, Macomb	New Jersey, Hunterdon
Connecticut, Middlesex	Connecticut, Middlesex	Michigan, Wayne	New Jersey, Gloucester
D.C., District of Columbia	D.C., District of Columbia	New Jersey, Hudson	New Jersey, Camden
Delaware, New Castle	Delaware, New Castle	New Jersey, Hunterdon	New Jersey, Middlesex
Georgia, DeKalb	Georgia, DeKalb	New Jersey, Gloucester	New Jersey, Mercer
Georgia, Rockdale	Georgia, Rockdale	New Jersey, Camden	New Jersey, Ocean
Georgia, Fulton	Georgia, Fulton	New Jersey, Middlesex	New York, Bronx
Indiana, Lake	Georgia, Henry	New Jersey, Mercer	New York, Westchester
Maryland, Baltimore	Maryland, Baltimore	New Jersey, Ocean	New York, Richmond

oxidant limited areas. But that is **not** what is happening in this case. The increase in ozone is caused by local predicted NO_X increases in the IPM model from certain power plants. These power plants were predicted to be controlled under the NO_X SIP call trading program (which is assumed in the 2010 Clear Skies base case). Under the Clear Skies control case, the plants trade under a new Clear Skies trading program which is year-round and expanded to additional states. The predicted emissions patterns from IPM are slightly different under the two trading programs. Therefore, some power plants that were predicted to put on controls under the NO_X SIP call may not be predicted to do so under Clear Skies (and vice versa). It is important to note that the overall summer utility NO_X emissions in the NO_X SIP call area are predicted to be lower under Clear Skies than under the NO_X SIP call. So overall, Clear Skies will provide regional ozone benefits in the NO_X SIP call area.

Maryland, Prince George's	Maryland, Prince George's	New York, Bronx	Pennsylvania , Montgomery
Maryland, Kent	Maryland, Kent	New York, Westchester	Pennsylvania , Bucks
Maryland, Anne Arundel	Maryland Anne Arundel	New York, Richmond	Texas, Galveston
Maryland, Harford	Maryland, Harford	Pennsylvania, Montgomery	Texas, Harris
Maryland, Cecil	Maryland, Cecil	Pennsylvania , Bucks	Wisconsin, Kenosha
New Jersey, Hudson	New Jersey, Hudson	Texas, Galveston	
New Jersey, Monmouth	New Jersey, Monmouth	Texas, Harris	
New Jersey, Cumberland	New Jersey, Morris	Wisconsin, Kenosha	
New Jersey, Morris	New Jersey, Hunterdon		
New Jersey, Hunterdon	New Jersey, Gloucester		
New Jersey, Gloucester	New Jersey, Camden		
New Jersey, Camden	New Jersey, Middlesex		
New Jersey, Middlesex	New Jersey, Mercer		
New Jersey, Mercer	New Jersey, Ocean		
New Jersey, Ocean	New York, Westchester		
New York, Erie	New York,Richmond		
New York, Westchester	North Carolina, Mecklenburg		
New York, Richmond	Pennsylvania, Delaware		
Pennsylvania, Delaware	Pennsylvania, Lancaster		
Pennsylvania, Lancaster	Pennsylvania, Lehigh		
Pennsylvania, Lehigh	Pennsylvania, Northampton		
Pennsylvania, Northampton	Pennsylvania, Montgomery		
Pennsylvania, Montgomery	Pennsylvania, Bucks		
Pennsylvania, Bucks	Rhode Island, Kent		
Rhode Island, Kent	Tennessee, Shelby		
Tennessee, Shelby	Texas, Tarrant		
Texas, Tarrant	Texas, Galveston		
Texas, Galveston	Texas, Collin		
Texas, Collin	Texas, Denton		
Texas, Denton	Texas, Harris		
Texas, Harris	Virginia, Fauquier		
Virginia, Caroline	Wisconsin, Kenosha		
Virginia, Fauquier	Wisconsin, Ozaukee		
Wisconsin, Door	Wisconsin, Sheboygan		
Wisconsin, Kenosha			
Wisconsin, Ozaukee			
Wisconsin, Sheboygan			
59 Counties	**56 Counties**	**30 Counties**	**27 Counties**

IV. Particulate Matter, Visibility, and Deposition Modeling over the Continental U.S.

A. REMSAD Model Description

The REgional Modeling System for Aerosols and Deposition (REMSAD) Version 7.06 (ICF Kaiser, 2002) model was used as the tool for simulating base year and future concentrations of PM, visibility, and deposition in support of the Clear Skies Act air quality assessments. Model runs were made for the 1996 and 2001 base years as well as for the 2010 and 2020 base and control scenarios. As described below, each of these emissions scenarios was simulated using 1996 meteorological data in order to provide the $PM_{2.5}$ concentrations needed for the nonattainment county analysis and annual mean PM concentrations, nitrogen, sulfur, and mercury deposition, and estimates of visibility needed for benefits calculations.

The basis for REMSAD is the atmospheric diffusion equation (also called the species continuity or advection/diffusion equation). This equation represents a mass balance in which all of the relevant emissions, transport, diffusion, chemical reactions, and removal processes are expressed in mathematical terms. REMSAD employs finite-difference numerical techniques for the solution of the advection/diffusion equation.

REMSAD was run using a latitude/longitude horizontal grid structure in which the horizontal grids are generally divided into areas of equal latitude and longitude. The vertical layer structure of REMSAD is defined in terms of sigma-pressure coordinates. The top and bottom of the domain are defined as 0 and 1 respectively. The vertical layers are defined as a percent of the atmospheric pressure between the top and bottom of the domain. For example, a vertical layer of 0.50 sigma is exactly halfway between the top and bottom of the domain as defined by the local atmospheric pressure. Usually, the vertical layers are defined to match the vertical layer structure of the meteorological model used to generate the REMSAD meteorological inputs.

1. Gas Phase Chemistry

REMSAD simulates gas phase chemistry using a reduced-form version of Carbon Bond (CB4) chemical mechanism termed "micro-CB4" (mCB4) which treats fewer VOC species compared to the full CB4 mechanism. The inorganic and radical parts of the reduced mechanism are identical to CB4. In this version of mCB4 the organic portion is based on three primary species (VOC, ISOP, and TERP) and one primary and secondary carbonyl species (CARB). The VOC species was incorporated with kinetics representing an average anthropogenic hydrocarbon species. The other two primary VOC species represent biogenic emissions of isoprene and terpenes and are included with kinetic characteristics representing isoprene and terpenes respectively. The intent of the mCB4 mechanism is to (a) provide a physically faithful representation of the linkages between emissions of ozone precursor species and secondary PM precursors species, (b) treat the oxidizing capacity of the troposphere, represented primarily by the concentrations of radicals and hydrogen peroxide, and (c) simulate the rate of oxidation of the nitrogen oxide (NO_X) and sulfur dioxide (SO_2) PM precursors. Box model testing of mCB4 has found that it performs very closely to the full CB4 that is contained in UAM-V (Whitten,

1999).

REMSAD version 7.06 includes several updates to the mCB4 mechanism relative to earlier versions of REMSAD. A new treatment for the NO_3 and N_2O_5 species has been implemented which results in improved agreement with rigorous solvers such as Gear and eliminates nitrogen mass inconsistencies. Also, several additional reactions have been added to the mCB4 mechanism which may be important for regional scale and annual applications where wide ranges in temperature, pressure, and concentrations may be encountered. The reactions are OH + H, OH + NO_3, and HO_2 + NO_3. For the same reason three reactions involving peroxy nitric acid (PNA), which were included in the original CB4 mechanism, were added to mCB4.

2. PM Chemistry

Primary PM emissions in REMSAD are treated as inert species. They are advected and deposited without any chemical interaction with other species. Secondary PM species, such as sulfate and nitrate are formed through chemical reactions within the model. SO_2 is the gas phase precursor for particulate sulfate, while nitric acid is the gas phase precursor for particulate nitrate. Several other gas phase species are also involved in the secondary reactions.

There are two pathways for sulfate formation; gas phase and aqueous phase. Aqueous phase reactions take place within clouds, rain, and/or fog. In-cloud processes can account for the majority of atmospheric sulfate formation in many areas. In REMSAD, aqueous SO_2 reacts with hydrogen peroxide (H_2O_2), ozone (O_3), and/or oxygen (O_2) to form aerosol sulfate. REMSAD version 7 has been upgraded to include all three aqueous phase sulfate reactions. Previous versions only contained the hydrogen peroxide reaction. The rate of the aqueous phase reactions depends on the concentrations of the chemical reactants as well as cloud water content. SO_2 also reacts with OH radicals in the gas phase to form aerosol sulfate. The aqueous phase and gas phase sulfate is typically added together to get the total sulfate concentration.

An equilibrium algorithm is used to calculate particulate nitrate concentrations. REMSAD version 7.06 uses the MARS-A equilibrium algorithm (Saxena et al., 1986) and (Kim et al., 1993). In REMSAD, particulate nitrate is calculated in an equilibrium reaction between nitric acid, sulfate, and ammonia. Nitric acid is a product of gas phase chemistry and is formed through the mCB4 reactions. The acids are neutralized by ammonia with sulfate reacting more quickly than nitric acid. An equilibrium is established among ammonium sulfate and ammonium nitrate which strongly favors ammonium sulfate. If the available ammonia exceeds twice the available sulfate then particulate nitrate is allowed to form as ammonium nitrate. Nitrate is then partitioned between particulate nitrate and gas phase nitric acid. The partitioning of nitrate depends on the availability of ammonia as well meteorological factors such as temperature and relative humidity.

An additional update to the REMSAD 7.06 code affects the dry deposition velocity of all gas phase species and in particular ammonia. Several assumptions contained in the REMSAD dry deposition code were removed. In previous versions of REMSAD, the surface resistance (Rc) for ammonia gas was set equal to 30 s/m at all times for the landuse categories of agriculture, range, and mixed agriculture and range. Additionally for the landuse types of deciduous forest, coniferous forest, and mixed forest, the ammonia surface resistance was set

equal to the stomatal resistance only . Both of these assumptions were removed from the code. The current version more closely follows the original work by Wesley (Wesley, 1989).

Organic aerosols can contribute a significant amount to the PM in the atmosphere. Primary organic aerosols (POA) are treated as a directly emitted species in REMSAD. In REMSAD version 7, a calculation of the production of secondary organic aerosols (SOA) due to atmospheric chemistry processes has been added[6]. A peer review of the REMSAD model (Seigneur et al., 1999) recommended an SOA module based on the equilibrium approach of Pankow (Odum et al., 1997), (Griffin et al., 1999). The implementation of the SOA treatment in version 7 of REMSAD follows the recommendation of the peer review. This includes SOA formation from anthropogenic and biogenic organic precursors. For both anthropogenic and biogenic organics REMSAD includes gas phase secondary organic species and the corresponding aerosol phase species.

B. REMSAD Modeling Domain

The REMSAD domain used for the Clear Skies modeling is shown in Figure IV-1. The geographic characteristics of the domain are as follows:

120 (E-W) X 84 (N-S) grid cells
Cell size (~36 km)
½ degree longitude (0.5)
1/3 degree latitude (0.3333)
E-W range: 66 degrees W - 126 degrees W
N-S range: 24 degrees N - 52 degrees N
Vertical extent: Ground to 16,200 meters (100mb) with 12 layers

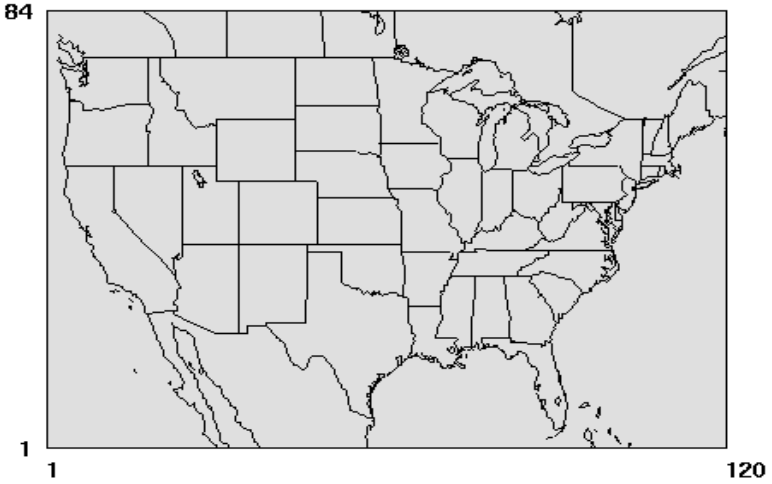

Figure IV-1. REMSAD Modeling Domain.

[6]An error was found in the SOA mechanism of REMSAD v7.01. This has been corrected in the current version (7.06). The reference temperature from the literature to calculate the partitioning coefficient (K) was assumed to be 298K when it should have been ~308K.

C. REMSAD Inputs

Input data for REMSAD can be classified into six categories: (1) simulation control, (2) emissions, (3) initial and boundary concentrations, (4) meteorological, (5) surface characteristics, and (6) chemical rates. The REMSAD predictions of pollutant concentrations are calculated from the emissions, advection, and dispersion processes coupled with the formation and deposition of secondary PM species within every grid cell of the modeling domain. To adequately replicate the full three-dimensional structure of the atmosphere, the REMSAD program uses hourly input data for a number of variables. Table IV-1 lists the required REMSAD input files.

Table IV-1. List of REMSAD input files.

Data type	Files	Description
Control	CONTROL	Simulation control information
Emissions	PTSOURCE EMISSIONS	Elevated source emissions Surface emissions
Initial and boundary concentrations	AIRQUALITY BOUNDARY	Initial concentrations Lateral boundary concentrations
Meteorological	WIND TEMPERATURE PSURF H2O VDIFFUSION RAIN	X,Y-components of winds 3D array of temperature 2D array of surface pressure 3D array of water vapor 3D array of vertical turbulent diffusivity coefficients 3D array of cloud water mixing ratio 3D array of rain water mixing ratio 2D array of rainfall rates
Surface characteristics	SURFACE TERRAIN	Gridded land use Terrain heights
Chemical rates	CHEMPARAM RATES	Chemical reaction rates Photolysis rates file

1. Meteorological Data

REMSAD requires input of winds (u- and v-vector wind components), temperatures, surface pressure, specific humidity, vertical diffusion coefficients, and rainfall rates. The meteorological input files were developed from a 1996 annual MM5 model run that was developed for previous projects. MM5 is the Fifth-Generation NCAR / Penn State Mesoscale Model. MM5 (Grell et al., 1994) is a numerical meteorological model that solves the full set of physical and thermodynamic equations which govern atmospheric motions. MM5 was run in a nested-grid mode with 2 levels of resolution: 108 km, and 36km with 23 vertical layers sigma layers extending from the surface to the 100 mb pressure level. The model was simulated in five day segments with an eight hour ramp-up period. The MM5 runs were started at 00Z, which is 7:00 p.m. EST. The first eight hours of each five day period were removed before being input into REMSAD. Figure IV-2 shows the MM5 and REMSAD 36km domain superimposed on each other. Table IV-2 lists the vertical grid structures for the MM5 and REMSAD domains. Further detailed information concerning the development and evaluation of the 1996 MM5 datasets can be found in (Olerud, 2000**).**

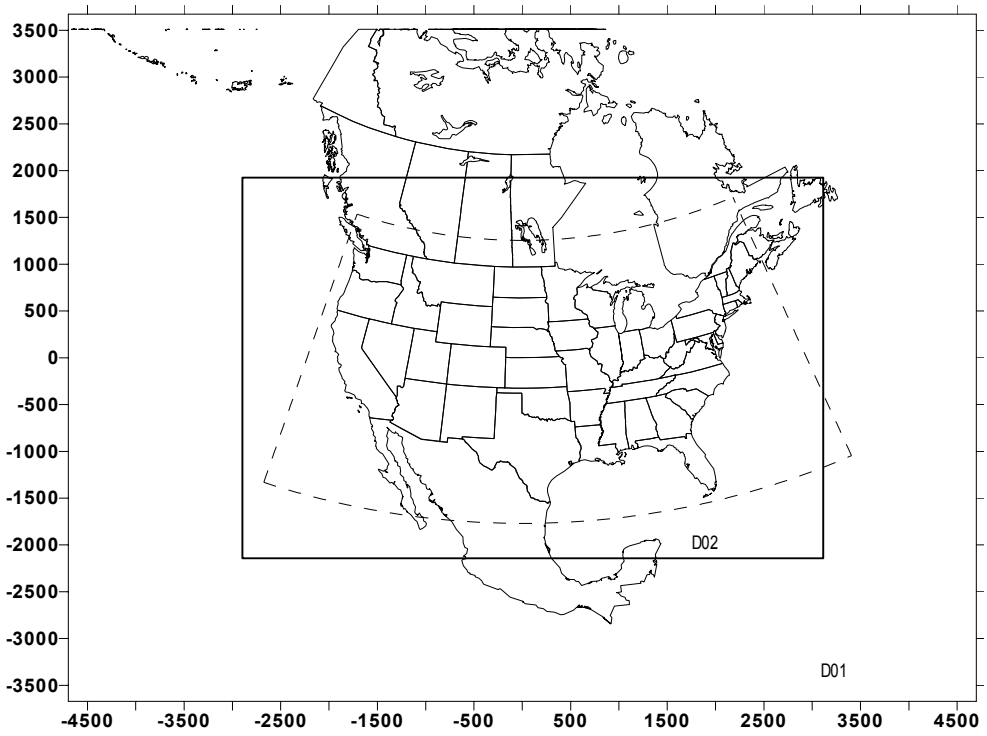

Figure IV-2. MM5 36km Domain (solid box) and REMSAD Domain (dashed lines).

Table IV-2. Vertical Grid Structure for 1996 MM5 and Clear Skies REMSAD Domains. Layer heights represent the top of each layer. The first layer is from the ground up to 38 meters.

REMSAD Layer	MM5 Layer	Sigma	Approximate Height(m)	Pressure(mb)
0	0	1.000	0.0	1000.0
1	1	0.995	38.0	995.5
2	2	0.988	91.5	989.2
	3	0.980	152.9	982.0
3	4	0.970	230.3	973.0
	5	0.956	339.5	960.4
4	6	0.938	481.6	944.2
	7	0.916	658.1	924.4
5	8	0.893	845.8	903.7
	9	0.868	1053.9	881.2
6	10	0.839	1300.7	855.1
	11	0.808	1571.4	827.2
7	12	0.777	1849.6	799.3
	13	0.744	2154.5	769.6
8	14	0.702	2556.6	731.8
	15	0.648	3099.0	683.2
9	16	0.582	3805.8	623.8
	17	0.500	4763.7	550.0
10	18	0.400	6082.5	460.0
	19	0.300	7627.9	370.0
11	20	0.200	9510.5	280.0
	21	0.120	11465.1	208.0
	22	0.052	13750.2	146.0
12	23	0.000	16262.4	100.0

The physical options selected for this configuration of MM5 include the following:

1. One-way nested grids
2. Nonhydrostatic dynamics
3. Four-dimensional data assimilation (FDDA):
    - Analysis nudging of wind, temperature, and mixing ratios
    - Nudging coefficients range from 1.0×10^{-5} s^{-1} to 3.0×10^{-4} s^{-1}
4. Explicit moisture treatment:
    - 3-D predictions of cloud and precipitation fields

- Simple ice microphysics (summer) and Mixed ice microphysics (winter)
- Cloud effects on surface radiation
- Moist vertical diffusion in clouds
- Normal evaporative cooling

5. Boundary conditions:
   - Time and inflow/outflow relaxation
6. Cumulus cloud parameterization schemes:
   - Anthes-Kuo (108-km grid)
   - Kain-Fritsch (36-km grid)
7. No shallow convection
8. Full 3-dimensional Coriolis force
9. Drag coefficients vary with stability
10. Vertical mixing of momentum in mixed layer
11. Virtual temperature effects
12. PBL process parameterization: MRF scheme
13. Surface layer parameterization:
    - Fluxes of momentum, sensible and latent heat
    - Ground temperature prediction using energy balance equation
    - 24 land use categories
14. Atmospheric radiation schemes:
    - Simple cooling
    - Long- and short-wave radiation scheme
15. Sea ice treatment:
    - Forced Great Lakes/Hudson Bay to permanent ice under very cold conditions
    - 36-km treatment keyed by observations of sea ice over the Great Lakes
16. Snow cover:
    - Assumed no snow cover for July and August
    - National Center for Environmental Prediction (NCEP) snow cover for January to June, and for September to December

The MM5 model output cannot be directly input into REMSAD due to differences in the grid coordinate systems and file formats. A postprocessor called MM5-REMSAD was developed to convert the MM5 data into REMSAD format. This postprocessor was used to develop hourly average meteorological input files from the MM5 output. Documentation of the MM5REMSAD code and further details on the development of the input files is contained in (Mansell, 2000).

2. Initial and Boundary Conditions, and Surface Characteristics

Application of the REMSAD modeling system requires data files specifying the initial species concentration fields (AIRQUALITY) and lateral species concentrations (BOUNDARY). Due to the extent of the proposed modeling domains and the regional-scale nature of the REMSAD model, these inputs were developed based on “clean” background concentration values. The Clear Skies modeling used temporally and spatially (horizontal) invariant data for both initial and boundary conditions. Species concentration values were allowed to decay

vertically for most species. Table IV-3 summarizes the initial and boundary conditions used in the Clear Skies REMSAD modeling.

Table IV-3. REMSAD Initial and Boundary Conditions (ppm)

	Layer 1	Layer 2	Layer 3	Layer 4	Layer 5	Layer 6	Layer 7	Layer 8	Layer 9	Layer 10	Layer 11	Layer 12
NO	1.00E-12	1.00E-12	1.00E-12	1.00E-12	1.00E-12	1.00E-12	1.00E-12	1.00E-12	8.44E-13	5.15E-13	1.72E-13	1.72E-13
NO2	1.00E-04	1.00E-04	1.00E-04	1.00E-04	1.00E-04	1.00E-04	1.00E-04	1.00E-04	8.44E-05	5.15E-05	1.72E-05	1.72E-05
O3	3.50E-02	3.50E-02	3.50E-02	3.50E-02	4.00E-02	4.00E-02	5.00E-02	5.00E-02	6.00E-02	6.00E-02	6.00E-02	7.00E-02
CO	8.00E-02	8.00E-02	8.00E-02	8.00E-02	8.00E-02	8.00E-02	8.00E-02	8.00E-02	8.00E-02	8.00E-02	8.00E-02	8.00E-02
SO2	3.00E-04	3.00E-04	3.00E-04	3.00E-04	3.00E-04	3.00E-04	3.00E-04	3.00E-04	2.53E-04	1.55E-04	5.15E-05	5.15E-05
NH3	1.00E-04	1.00E-04	1.00E-04	1.00E-04	1.00E-04	1.00E-04	1.00E-04	1.00E-04	7.12E-05	2.66E-05	2.95E-06	2.95E-06
VOC	2.00E-02	2.00E-02	2.00E-02	2.00E-02	2.00E-02	2.00E-02	2.00E-02	2.00E-02	1.69E-02	1.03E-02	3.44E-03	3.44E-03
CARB	1.00E-07	1.00E-07	1.00E-07	1.00E-07	1.00E-07	1.00E-07	1.00E-07	1.00E-07	1.00E-07	1.00E-07	1.00E-07	1.00E-07
ISOP	1.00E-09	1.00E-09	1.00E-09	1.00E-09	1.00E-09	1.00E-09	1.00E-09	1.00E-09	1.00E-09	1.00E-09	1.00E-09	1.00E-09
HNO3	1.00E-05	1.00E-05	1.00E-05	1.00E-05	1.00E-05	1.00E-05	1.00E-05	1.00E-05	8.44E-06	5.15E-06	1.72E-06	1.72E-06
PNO3	1.00E-05	1.00E-05	1.00E-05	1.00E-05	1.00E-05	1.00E-05	1.00E-05	1.00E-05	7.12E-06	2.66E-06	2.95E-07	2.95E-07
HG0	1.95E-07	1.95E-07	1.95E-07	1.95E-07	1.95E-07	1.95E-07	1.95E-07	1.95E-07	1.39E-07	5.18E-08	5.76E-09	5.76E-09
HG2G	9.75E-09	9.75E-09	9.75E-09	9.75E-09	9.75E-09	9.75E-09	9.75E-09	9.75E-09	6.94E-09	1.59E-09	2.88E-10	2.88E-10
GSO4	1.00E-05	1.00E-05	1.00E-05	1.00E-05	1.00E-05	1.00E-05	1.00E-05	1.00E-05	7.12E-06	2.66E-06	2.95E-07	2.95E-07
ASO4	1.00E-12	1.00E-12	1.00E-12	1.00E-12	1.00E-12	1.00E-12	1.00E-12	1.00E-12	7.12E-13	2.66E-13	2.95E-14	2.95E-14
NH4N	1.00E-05	1.00E-05	1.00E-05	1.00E-05	1.00E-05	1.00E-05	1.00E-05	1.00E-05	7.12E-06	2.66E-06	2.95E-07	2.95E-07
NH4S	1.00E-05	1.00E-05	1.00E-05	1.00E-05	1.00E-05	1.00E-05	1.00E-05	1.00E-05	7.12E-06	2.66E-06	2.95E-07	2.95E-07
SOA	1.00E-03	1.00E-03	1.00E-03	1.00E-03	1.00E-03	1.00E-03	1.00E-03	1.00E-03	7.12E-04	2.66E-04	2.95E-05	2.95E-05
POA	1.00E-03	1.00E-03	1.00E-03	1.00E-03	1.00E-03	1.00E-03	1.00E-03	1.00E-03	7.12E-04	2.66E-04	2.95E-05	2.95E-05
PEC	1.00E-03	1.00E-03	1.00E-03	1.00E-03	1.00E-03	1.00E-03	1.00E-03	1.00E-03	7.12E-04	2.66E-04	2.95E-05	2.95E-05
PMFINE	1.00E-03	1.00E-03	1.00E-03	1.00E-03	1.00E-03	1.00E-03	1.00E-03	1.00E-03	7.12E-04	2.66E-04	2.95E-05	2.95E-05
PMCOARS	1.00E-03	1.00E-03	1.00E-03	1.00E-03	1.00E-03	1.00E-03	1.00E-03	1.00E-03	6.00E-04	1.37E-04	5.07E-06	5.07E-06
HG2P	1.22E-09	1.22E-09	1.22E-09	1.22E-09	1.22E-09	1.22E-09	1.22E-09	1.22E-09	8.54E-10	3.19E-10	3.54E-11	3.54E-11

Application of the REMSAD model requires specification of gridded terrain elevations (TERRAIN) and landuse characteristics (SURFACE). The SURFACE data files provides the fraction of the 11 landuse categories recognized by REMSAD in each grid cell. Landuse characteristics are used in the model for the calculation of deposition parameters. For this task, a landuse/terrain processor, PROC_LUTERR, was developed based on the MM5 TERRAIN preprocessor. Landuse data was obtained from the USGS Global 30 sec. vegetation database which is the same database used in the 1996 MM5 models runs. This dataset provides 24 landuse categories, including urban. For the REMSAD application, the 10 min. (1/6 deg.) datasets was utilized. The processor remapped the 24 USGS vegetation categories to those required for application of REMSAD. It also aggregated the 10 min resolution data to the ~36 km horizontal resolution used for this REMSAD application.

For the TERRAIN input data files, a similar global terrain elevation dataset is also available from NCAR and was used for this task. While it is possible to use the terrain elevations obtained from the MM5 model output data files, it was deemed more appropriate to

begin with the USGS 10 min. resolution database due to the various map projections and interpolations involved in developing the required data files for the geodetic coordinates used in REMSAD. However, because proper application of REMSAD will require zero terrain elevations, "dummy" terrain files (with all zeroes) were developed and provided for input to REMSAD.

D. Model Performance Evaluation

The goal of the 1996 Base Year modeling was to reproduce the atmospheric processes resulting in formation and dispersion of fine particulate matter across the U.S. An operational model performance evaluation for $PM_{2.5}$ and its related speciated components (e.g., sulfate, nitrate, elemental carbon etc.) for 1996 was performed in order to estimate the ability of the modeling system to replicate Base Year concentrations.

This evaluation is comprised principally of statistical assessments of model versus observed pairs. The robustness of any evaluation is directly proportional to the amount and quality of the ambient data available for comparison. Unfortunately, there are few $PM_{2.5}$ monitoring networks with available data for evaluation of the Clear Skies PM modeling. Critical limitations of the 1996 databases are a lack of urban monitoring sites with speciated measurements and poor geographic representation of ambient concentration in the East. $PM_{2.5}$ monitoring networks were expanded in 1999 to include more than 1000 Federal Reference Method (FRM) monitoring sites. The purpose of this network is to monitor $PM_{2.5}$ mass levels in urban areas. These monitors only measure total $PM_{2.5}$ mass and do not measure PM species. In 2001 a new network of ~300 urban oriented speciation monitor sites began operation across the country. These monitors collect a full range of $PM_{2.5}$ species that are necessary to evaluate models and to develop $PM_{2.5}$ control strategies. Future modeling efforts will be able to take advantage of these newer speciated $PM_{2.5}$ measurements.

The evaluation used data from the IMPROVE, CASTNet dry deposition, and NADP monitoring networks (IMPROVE, 2000), (EPA, 2002), (NADP, 2003). The IMPROVE and NADP networks were in full operation during 1996. The CASTNet dry deposition network was partially shutdown during the first half of the year. There were 65 CASTNet sites with at least one season of complete data. There were 16 sites which had complete annual data. The CASTNet visibility network was also partially operating in 1996. Data from the 7 visibility sites is only complete from September-December. This only provides a single season (fall) of complete data. Therefore, the limited data from these sites was not used in the evaluation. The mercury deposition network (MDN) was in its first year of operation in 1996. There was not adequate data to fully evaluate the wet deposition of total mercury.

The largest available ambient database for 1996 comes from the **I**nteragency **M**onitoring of **PRO**tected **V**isual **E**nvironments (IMPROVE) network. IMPROVE is a cooperative visibility monitoring effort between EPA, federal land management agencies, and state air agencies. Data is collected at Class I areas across the United States mostly at National Parks, National Wilderness Areas, and other protected pristine areas. There were approximately 60 IMPROVE sites that had complete annual $PM_{2.5}$ mass and/or $PM_{2.5}$ species data for 1996. Forty two sites

were in the West[7] and 18 sites were in the East. Figure IV-3 shows the locations of the IMPROVE monitoring sites used in this evaluation. IMPROVE data is collected twice weekly (Wednesday and Saturday). Thus, there is a total of 104 possible samples per year or 26 samples per season. For this analysis, a 50% completeness criteria was used[8]. That is, in order to be counted in the statistics a site had to have > 50% complete data in all 4 seasons. If any season was missing, an annual average was not calculated for the site. See Appendix D for a list of the IMPROVE sites used in the evaluation. The observed IMPROVE data used for the performance evaluation was $PM_{2.5}$ mass, sulfate ion, nitrate ion, elemental carbon, organic aerosols, and crustal material (soils). The REMSAD model output species were postprocessed in order to achieve compatibility with the observation species. The following is the translation of REMSAD output species into $PM_{2.5}$ and related species:

Sulfate Ion:	TSO4 = ASO4 + GSO4
Nitrate Ion:	PNO3
Organic aerosols:	TOA = 1.167*POA + SOA1 + SOA2 + SOA3 + SOA4
Elemental Carbon:	PEC
Crustal Material (soils):	PMFINE
$PM_{2.5}$:	$PM_{2.5}$ = PMFINE + ASO4 + GSO4 + NH4S + PNO3 + NH4N + 1.167*POA + PEC + SOA1 + SOA2 + SOA3 + SOA4

where, TSO4 is total sulfate ion, ASO4 is aqueous path sulfate, GSO4 is gaseous path sulfate, NH4S is ammonium associated with sulfate, PNO3 is nitrate ion, NH4N is ammonium associated with nitrate, TOA is total organic aerosols, POA is primary organic aerosol[9], SOA1 and SOA2 are anthropogenic secondary organic aerosol, SOA3 and SOA4 are biogenic secondary organic aerosol, PEC is primary elemental carbon, and PMFINE is primary fine particles (other unspeciated primary $PM_{2.5}$). $PM_{2.5}$ is defined as the sum of the individual species.

[7]The dividing line between the West and East was defined as the 100th meridian.

[8]The same completeness criteria was used for all of the monitoring networks.

[9]For the performance evaluation and the calculation of $PM_{2.5}$ mass, POA is multiplied by 1.167. The IMPROVE organic carbon mass is multiplied by a 1.4 factor to account for additional mass attached to the carbon (this follows standard IMPROVE procedures). In REMSAD, the "additional" mass is already accounted for in the SOA predictions (by using a molecular weight of 160 g/mole). The POA emissions have been multiplied by1.2 prior to processing by the emissions model (the 1.2 factor is applied to the organic carbon in the $PM_{2.5}$ speciation profiles). The post-processed POA concentrations are then multiplied by 1.167 to simulate an equivalent 1.4 factor (1.2 * 1.167 = 1.4).

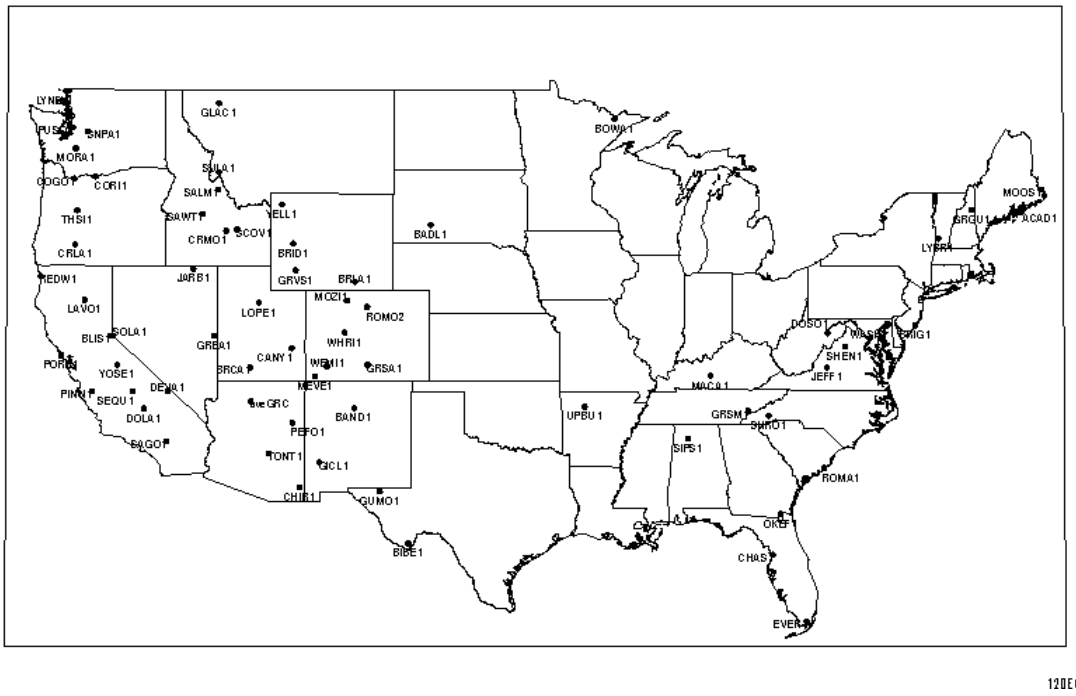

12DEC00

Figure IV-3. Map of 1996 IMPROVE monitoring sites used in the REMSAD model performance evaluation.

Model performance was also calculated using data from the CASTNet dry deposition monitoring network. The sulfate and total nitrate data was used in the evaluation. CASTNet data is collected and reported as weekly average data. The data is collected in filter packs that sample the ambient air continuously during the week. The sulfate data is of high quality since sulfate is a very stable compound. But the particulate nitrate concentration data collected by CASTNet is subject to volatility due to the length of the sampling period. Therefore, we chose not to use the CASTNet particulate nitrate data in this evaluation. CASTNet also reports a total nitrate measurement. This is the combined total of particulate nitrate and nitric acid. Since the total nitrate measurement is not affected by the partitioning back and forth between particulate nitrate and nitric acid, it should be a fairly accurate measurement.

Wet deposition data from the National Acid Deposition Program (NADP) was also used in the model evaluation. There were a total of 160 NADP sites with complete annual data in 1996. Model results were compared to observed values of ammonium, sulfate, and nitrate wet deposition.

1. Statistical Definitions

Below are the definitions of statistics used for the evaluation. The format of all the statistics is such that negative values indicate model predictions that were less than their observed counterparts. Positive statistics indicate model overestimation of observed PM.. The statistics were calculated for the entire REMSAD domain and separated for the east and the west. The dividing line between East and West is the 100th meridian.

Mean Observation: The mean observed value (in μg/m^3) averaged over all monitored days in the year and then averaged over all sites in the region.

$$OBS = \frac{1}{N} \sum_{i=1}^{N} Obs_{x,t}^{i}$$

Mean REMSAD Prediction: The mean predicted value (in μg/m^3) paired in time and space with the observations and then averaged over all sites in the region.

$$PRED = \frac{1}{N} \sum_{i=1}^{N} Pred_{x,t}^{i}$$

Ratio of the Means: Ratio of the predicted over the observed values. A ratio of greater than 1 indicates on overprediction and a ratio of less than 1 indicates an underprediction.

$$RATIO = \frac{1}{N} \sum_{i=1}^{N} \frac{Pred_{x,t}^{i}}{Obs_{x,t}^{i}}$$

Mean Bias (μg/m^3): This performance statistic averages the difference (model - observed) over all pairs in which the observed values were greater than zero. A mean bias of zero indicates that the model over predictions and model under predictions exactly cancel each other out. Note that the model bias is defined such that it is a positive quantity when model prediction exceeds the observation, and vice versa. This model performance estimate is used to make statements about the absolute or unnormalized bias in the model simulation

$$BIAS = \frac{1}{N} \sum_{i=1}^{N} (Pred_{x,t}^{i} - Obs_{x,t}^{i})$$

Mean Fractional Bias (percent): Normalized bias can become very large when a minimum threshold is not used. Therefore fractional bias is used as a substitute. The fractional bias for cases with factors of 2 under- and over-prediction are -67 and + 67 percent, respectively (as opposed to -50 and +100 percent, when using normalized bias, which is not presented here).

Fractional bias is a useful model performance indicator because it has the advantage of equally weighting positive and negative bias estimates. The single largest disadvantage in this estimate of model performance is that the estimated concentration (i.e., prediction, Pred) is found in both the numerator and denominator.

$$FBIAS = \frac{2}{N} \sum_{i=1}^{N} \frac{(Pred_{x,t}^{i} - Obs_{x,t}^{i})}{(Pred_{x,t}^{i} + Obs_{x,t}^{i})} * 100$$

Mean Error (μg/m^3): This performance statistic averages the absolute value of the difference (model - observed) over all pairs in which the observed values were greater than zero. It is similar to mean bias except that the absolute value of the difference is used so that the error is always positive.

$$ERR = \frac{1}{N} \sum_{i=1}^{N} |Pred_{x,t}^{i} - Obs_{x,t}^{i}|$$

Mean Fractional Error (percent): Normalized error can become very large when a minimum threshold is not used. Therefore fractional error is used as a substitute. It is similar to the fractional bias except the absolute value of the difference is used so that the error is always positive.

$$FERROR = \frac{2}{N} \sum_{i=1}^{N} \frac{|Pred_{x,t}^{i} - Obs_{x,t}^{i}|}{Pred_{x,t}^{i} + Obs_{x,t}^{i}} * 100$$

Correlation Coefficient: This performance statistic measures the degree to which two variables are linearly related. A correlation of coefficient of 1 indicates a perfect linear relationship, whereas a correlation coefficient of 0 means that there is no linear relationship between the variables.

$$CORRCOEFF = \frac{\sum_{i=1}^{N} (Pred_i - \overline{Pred})\,(Obs_i - \overline{Obs})}{\sqrt{\sum_{i=1}^{N} (Pred_i - \overline{Pred})^2 \sum_{i=1}^{N} (Obs_i - \overline{Obs})^2}}$$

2. Results of REMSAD Performance Evaluation

The statistics described above are presented for the entire domain, the Eastern sites, and the Western sites. The statistics were calculated in two different ways. The bias, error, and R^2 statistics in the **tables** below were calculated for all days and all sites. Observations and model predictions were paired in time and space on a daily basis. These statistics represent the ability of the model to replicate each day of year with measurements.

Following the statistical tables are scatterplots of seasonal and annual average predictions at each ambient data site. These scatterplots represent the ability of the model to represent a seasonal average or annual average measurement. The correlation coefficients for the scatterplots represent the correlation of the site average (seasonal and/or annual) predictions to the site average measurements.

a. IMPROVE Performance

a.1. $PM_{2.5}$ Performance

Table IV-4 lists the performance statistics for $PM_{2.5}$ at the IMPROVE sites. For the full domain, $PM_{2.5}$ is underpredicted by 18%. Overall, the performance of REMSAD (v7.06) has improved from underpredicting $PM_{2.5}$ by 34% in version 7.01. The ratio of the means is 0.82 with a bias of -1.10 $\mu g/m^3$. It can be seen that most of this underprediction is due to the Western sites. The West is underpredicted by 33% while the East is underpredicted by 2%. The fractional bias is ~9% in the East, while the fractional error is 46%. The fractional bias and error in the West is ~30% and 63% respectively. The observed $PM_{2.5}$ concentrations in the East are relatively high compared to the West. REMSAD displays an ability to differentiate between generally high and low $PM_{2.5}$ areas.

Table IV-4. Annual mean $PM_{2.5}$ performance at IMPROVE sites.

	No. of Sites	Mean REMSAD Predictions ($\mu g/m^3$)	Mean Observations ($\mu g/m^3$)	Ratio of Means (pred/obs)	Bias ($\mu g/m^3$)	Fractional Bias (%)	Error ($\mu g/m^3$)	Fractional Error (%)	Correlation Coefficient
National	54	5.11	6.21	0.82	-1.10	-24.1	3.01	58.2	0.46
East	15	10.93	11.15	0.98	-0.22	-8.9	4.99	46.1	0.39
West	39	2.87	4.31	0.67	-1.44	-29.9	2.44	62.8	0.09

Figures IV-4 and IV-5 show the annual and seasonal average $PM_{2.5}$ 1996 IMPROVE observations versus REMSAD predictions respectively. The annual and seasonal scatterplots showed some scatter, but good agreement, with strong correlations (annual: $R^2 = 0.79$; summer: $R^2 = 0.69$; fall: $R^2 = 0.62$; spring: $R^2 = 0.60$; and winter: $R^2 = 0.78$).

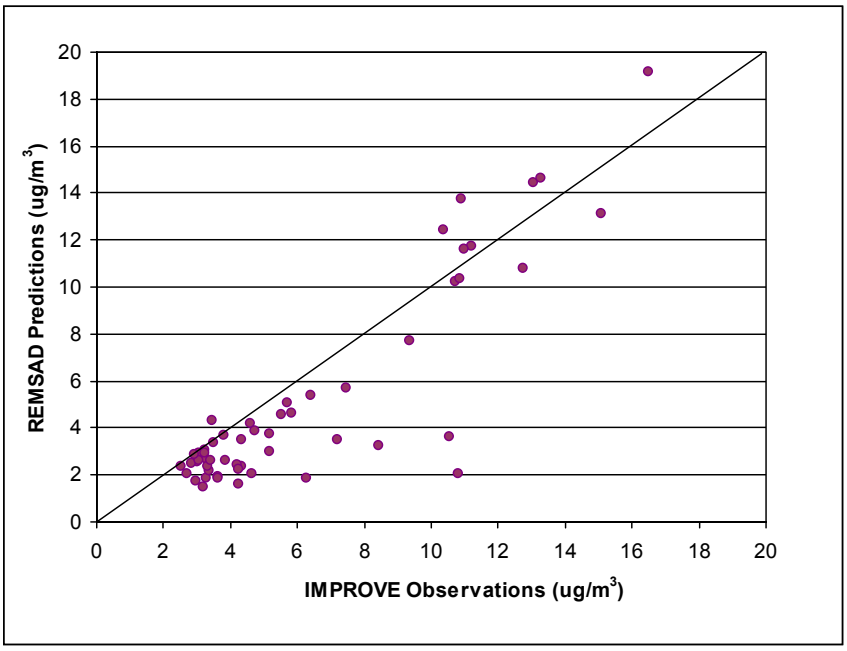

Figure IV-4. Annual average $PM_{2.5}$ 1996 IMPROVE observations versus REMSAD predictions.

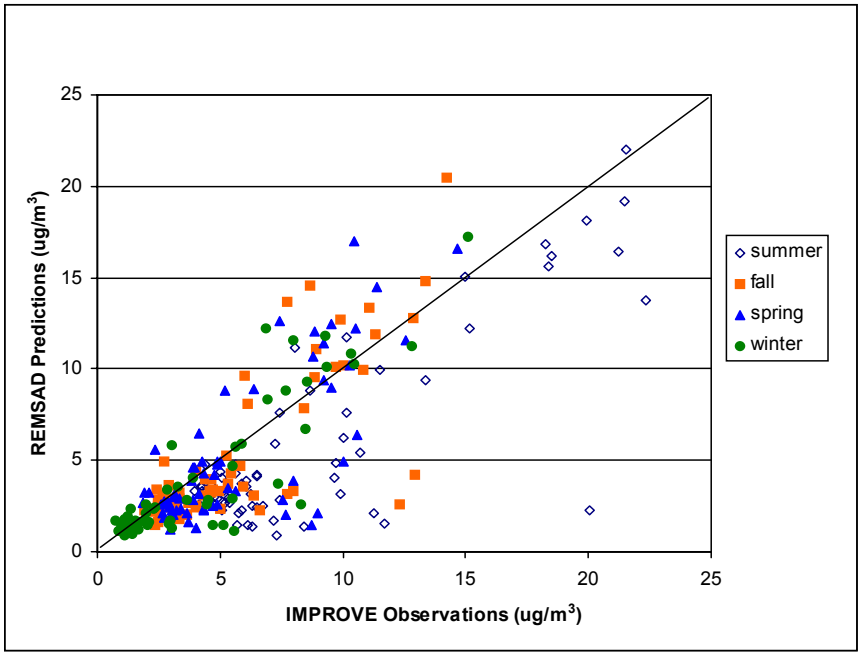

Figure IV-5. Seasonal average $PM_{2.5}$ 1996 IMPROVE observations versus REMSAD predictions

a.2. Sulfate Performance

Table IV-5 lists the performance statistics for particulate sulfate at the IMPROVE sites. Domainwide, sulfate is underpredicted by 21%. The annual average sulfate underprediction in the east is 12% and 41% in the West. The sulfate performance (especially in the East) is better than most of the other PM2.5 species. The fractional error in the East is ~60% and the R^2 is 0.51.

Table IV-5. Annual mean sulfate ion performance at IMPROVE sites.

	No. of Sites	Mean REMSAD Predictions ($\mu g/m^3$)	Mean Observations ($\mu g/m^3$)	Ratio of Means (pred/obs)	Bias ($\mu g/m^3$)	Fractional Bias (%)	Error ($\mu g/m^3$)	Fractional Error (%)	Correlation Coefficient
National	58	1.25	1.59	0.79	-0.34	-40.7	0.80	69.3	0.66
East	16	3.47	3.93	0.88	-0.46	-29.8	1.80	60.2	0.51
West	42	0.41	0.69	0.59	-0.29	-44.8	0.41	72.8	0.13

Figures IV-6 and IV-7 show the annual and seasonal average sulfate 1996 IMPROVE observations versus REMSAD predictions respectively. The scatterplots and linear regressions displayed strong correlations (annual: $R^2 = 0.96$; summer: $R^2 = 0.92$; fall: $R^2 = 0.91$; spring: $R^2 = 0.90$; and winter: $R^2 = 0.86$).

Overall, the model shows an ability to replicate the annual and seasonal sulfate concentrations. This is particularly important for this application of REMSAD. The Clear Skies emissions controls mainly reduce SO_2 and lead to large predicted sulfate reductions. It is important to have good model performance for the species that is being reduced the most.

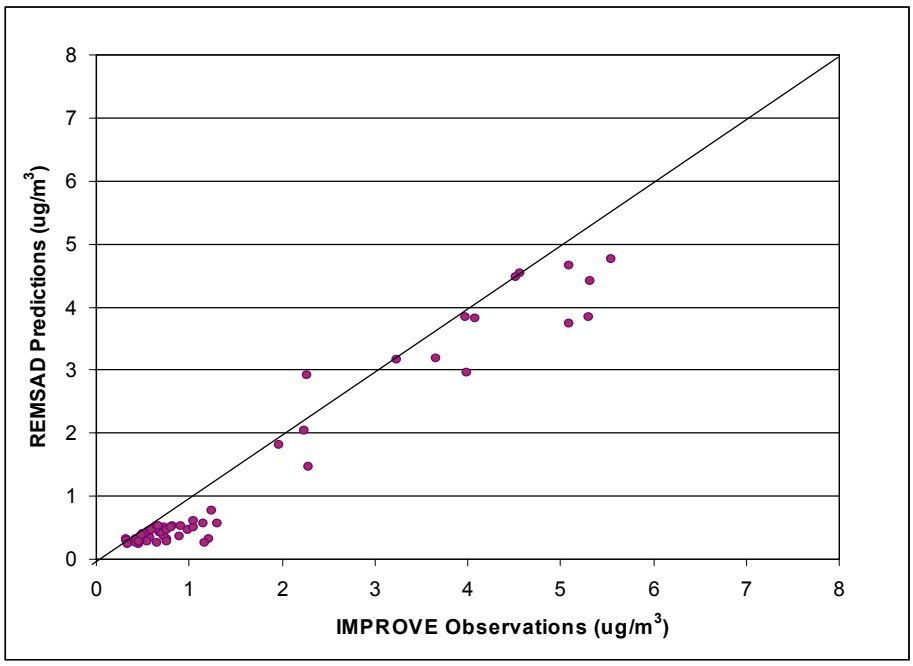

Figure IV-6. Annual average sulfate 1996 IMPROVE observations versus REMSAD predictions.

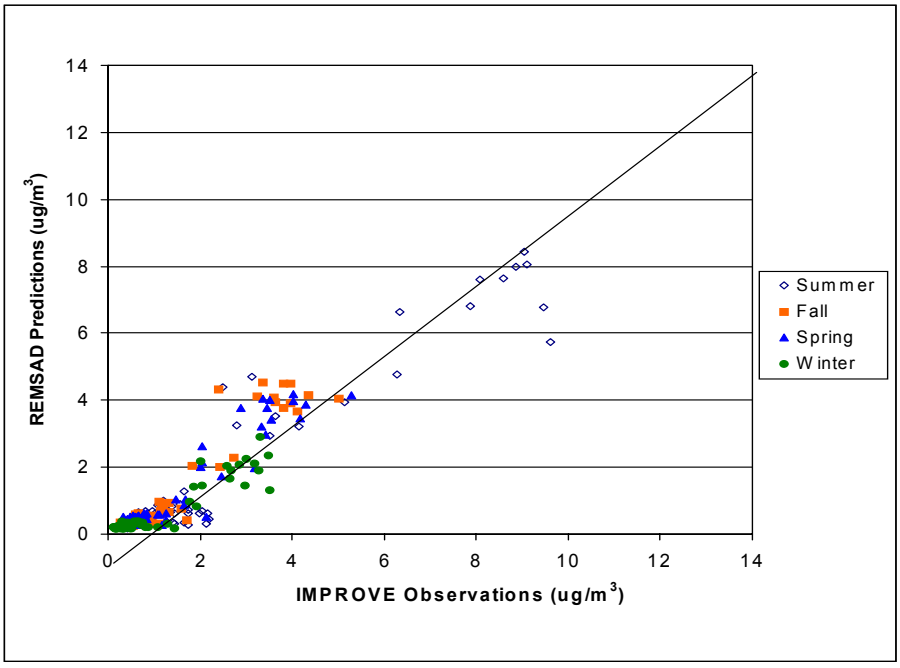

Figure IV-7. Seasonal average sulfate 1996 IMPROVE observations versus REMSAD predictions.

a.3. Elemental Carbon Performance

Table IV-6 lists the performance statistics for primary elemental carbon at the IMPROVE sites. Elemental carbon concentrations at IMPROVE sites are relatively low, but performance is generally good. There is a domainwide underprediction of 14% and a western underprediction of 29%.

Table IV-6. Annual mean elemental carbon performance at IMPROVE sites.

	No. of Sites	Mean REMSAD Predictions ($\mu g/m^3$)	Mean Observations ($\mu g/m^3$)	Ratio of Means (pred/obs)	Bias ($\mu g/m^3$)	Fractional Bias (%)	Error ($\mu g/m^3$)	Fractional Error (%)	Correlation Coefficient
National	47	0.27	0.32	0.86	-0.05	-13.6	0.17	58.7	0.33
East	15	0.49	0.48	1.01	0.01	1.78	0.20	41.7	0.47
West	32	0.17	0.24	0.71	-0.07	-20.9	0.16	66.7	0.07

Figures IV-8 and IV-9 show scatterplots of annual and seasonal average elemental carbon 1996 IMPROVE observations versus REMSAD predictions respectively. The annual scatterplot and linear regression displayed some scatter, however good agreement with a R^2 of 0.53. Overall, summer and fall linear regressions had relatively good agreement (summer: $R^2 = 0.63$; fall: $R^2 = 0.62$), whereas spring and winter had the weakest correlations (spring: $R^2 = 0.49$; and winter: $R^2 = 0.39$).

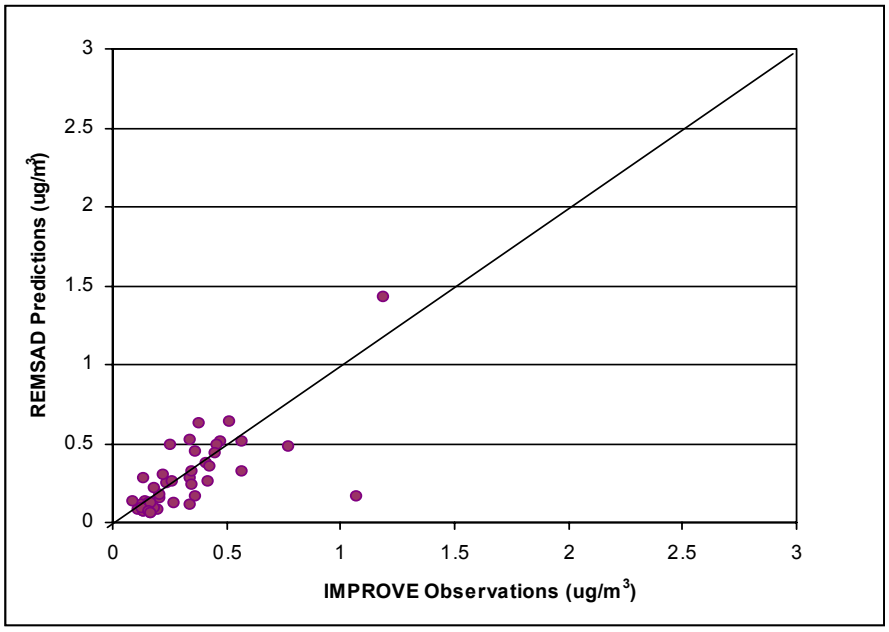

Figure IV-8. Annual average elemental carbon 1996 IMPROVE observations versus REMSAD predictions.

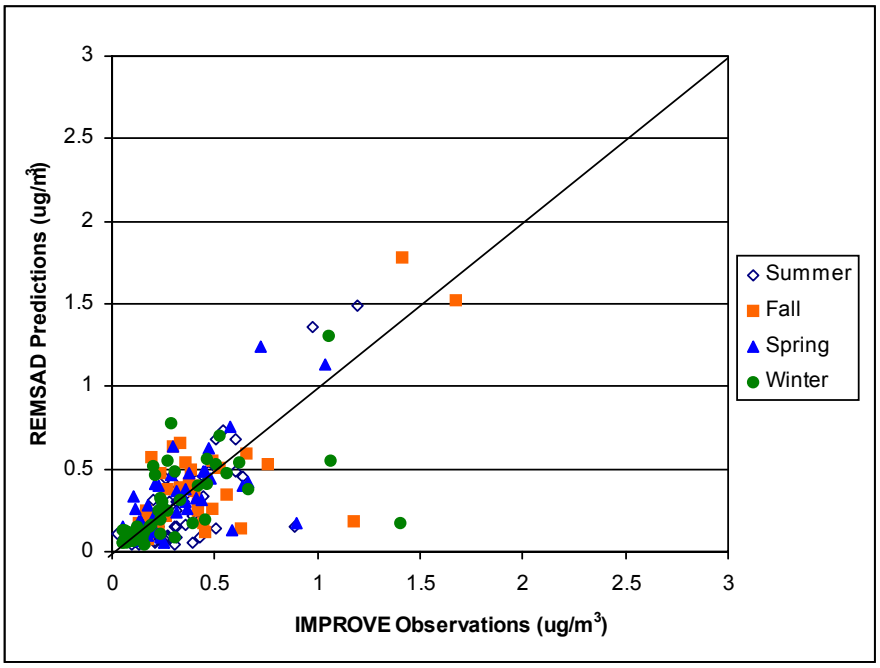

Figure IV-9. Seasonal average elemental carbon 1996 IMPROVE observations versus REMSAD predictions.

a.4. Organic Aerosol Performance

Table IV-7 lists the performance statistics for organic aerosols at the IMPROVE sites. Organic aerosols performance is generally good. The nationwide bias and errors are low. But the correlation coefficient is also low. There is much uncertainty in the predictions of organic carbon. There are several different forms of organic carbon predicted in the model. There is primary organic carbon, secondary biogenic organic carbon, and secondary anthropogenic organic carbon. Both the model and the ambient data contains a mix of these different types of organics which all originate from different sources. Unfortunately, given limitations in measurement techniques, it is currently not possible to quantify the different types of organic carbon in the ambient air.

This latest version of REMSAD (7.06) contains science updates and code fixes that result in predicted concentrations of secondary organic carbon that are much higher than in previous versions of REMSAD. The model predictions for organics are tempered by the fact that wildfires (a significant source of organic carbon) are not included in the current modeling inventory. The performance for organics should be viewed relative to the uncertainties in the measurements and the emissions inventories.

Table IV-7. Annual mean organic aerosol performance at IMPROVE sites.

	No. of Sites	Mean REMSAD Predictions ($\mu g/m^3$)	Mean Observations ($\mu g/m^3$)	Ratio of Means (pred/obs)	Bias ($\mu g/m^3$)	Fractional Bias (%)	Error ($\mu g/m^3$)	Fractional Error (%)	Correlation Coefficient
National	47	1.76	1.76	1.00	0.004	-5.58	1.13	62.0	0.18
East	15	2.58	2.49	1.04	0.09	-11.83	1.42	54.7	0.21
West	32	1.38	1.42	0.97	-0.04	-2.64	1.00	65.4	0.10

Annual and seasonal scatterplots (Figures IV-10 and IV-11) of average organic aerosol for 1996 IMPROVE observations versus REMSAD predictions displayed some scatter, with an annual $R^2 = 0.40$ and seasonal correlations of: summer: $R^2 = 0.43$; fall: $R^2 = 0.23$; spring: $R^2 = 0.45$; and winter: $R^2 = 0.45$.

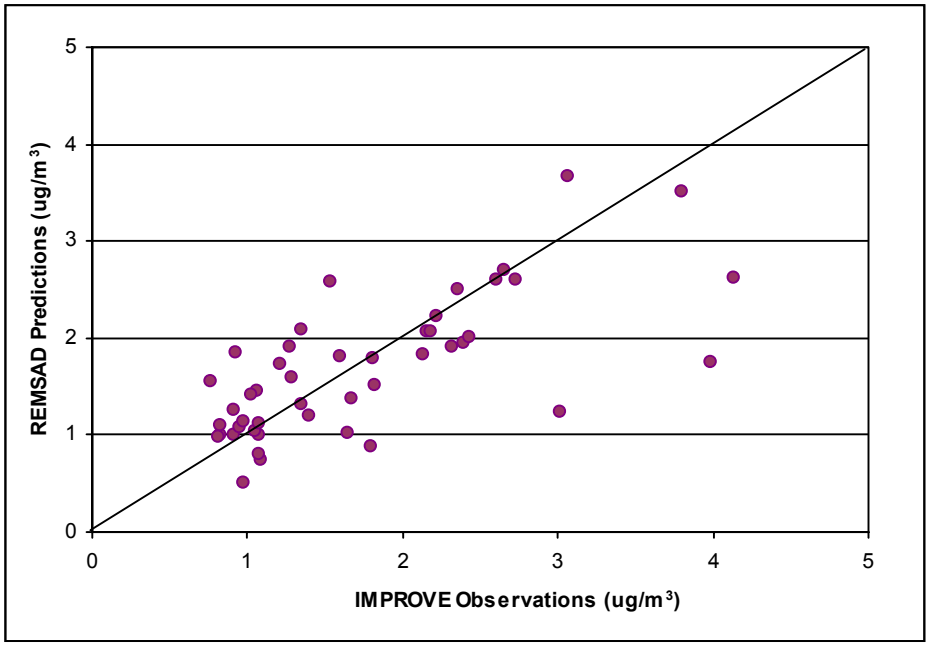

Figure IV-10. Annual average organic aerosol 1996 IMPROVE observations versus REMSAD predictions.

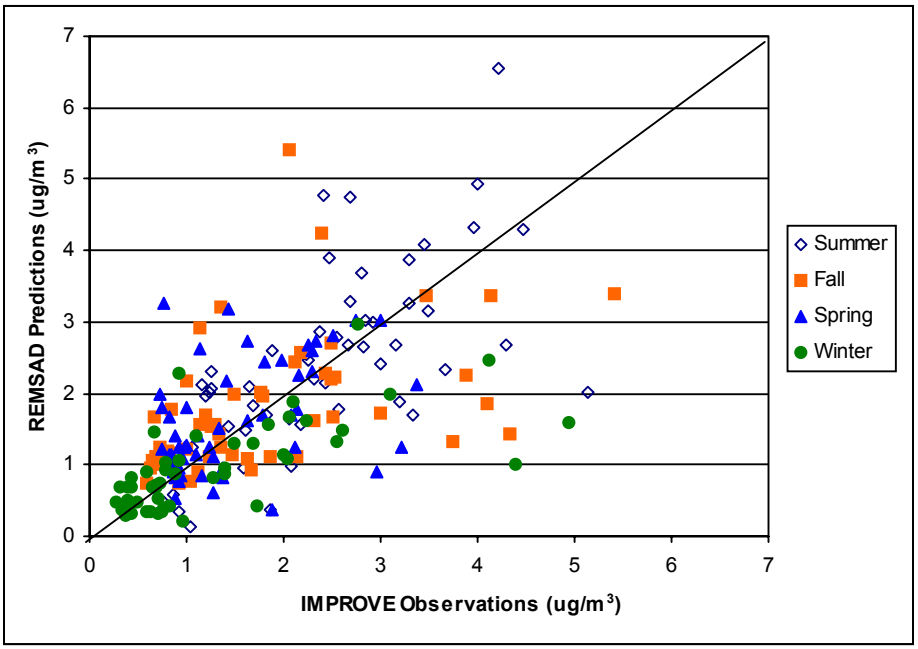

Figure IV-11. Seasonal average organic aerosol 1996 IMPROVE observations versus REMSAD predictions.

a.5. Nitrate Performance

Table IV-8 lists the performance statistics for nitrate ion at the IMPROVE sites. Nitrate is generally overpredicted in the East and underpredicted in the West. Nitrate is overpredicted by 166% in the east and underpredicted by 31% in the west. Domainwide there is an overprediction of 55%.

Table IV-8. Annual mean nitrate ion performance at IMPROVE sites.

	No. of Sites	Mean REMSAD Predictions ($\mu g/m^3$)	Mean Observations ($\mu g/m^3$)	Ratio of Means (pred/obs)	Bias ($\mu g/m^3$)	Fractional Bias (%)	Error ($\mu g/m^3$)	Fractional Error (%)	Correlation Coefficient
National	48	0.61	0.39	1.55	0.21	-59.4	0.57	129.8	0.19
East	15	1.47	0.55	2.66	0.91	13.0	1.11	109.3	0.29
West	33	0.22	0.32	0.69	-0.10	-91.9	0.32	139.0	0.15

Likewise, this overprediction is depicted in Figures IV-12 and IV-13, which show the scatterplots of the annual (R^2= 0.37) and seasonal (summer: R^2= 0.24; fall: R^2= 0.17; spring: R^2= 0.36; winter: R^2= 0.52) average nitrate ion for 1996 IMPROVE observations verus REMSAD predictions.

It is important to consider these results in the context that the observed nitrate concentrations at the IMPROVE sites are very low. The mean nationwide observations are only 0.40 μg/m^3. It is often difficult for models to replicate very low concentrations of secondarily formed pollutants. Nitrate is generally a small percentage of the measured $PM_{2.5}$ at almost all of the IMPROVE sites. Nonetheless, it has been recognized that the current generation of PM air quality models generally overpredict particulate nitrate. There are numerous ongoing efforts to improve particulate nitrate model performance through emissions inventory improvements (ammonia emissions and dry deposition of gaseous precursors) and improvements in the scientific formulations of the models.

More recent ambient data has shown that nitrate can be an important contributor to $PM_{2.5}$ in some urban areas (particularly in California and the upper Midwest) but performance for those areas could not be assessed due to the lack of urban area speciated nitrate data for 1996.

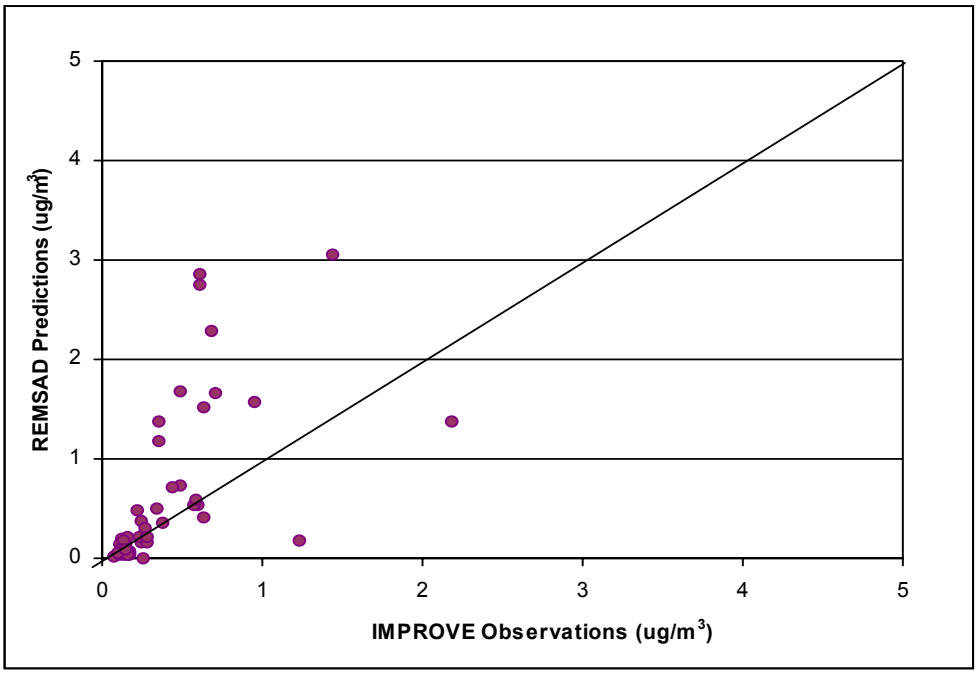

Figure IV-12. Annual average nitrate ion 1996 IMPROVE observations versus REMSAD predictions.

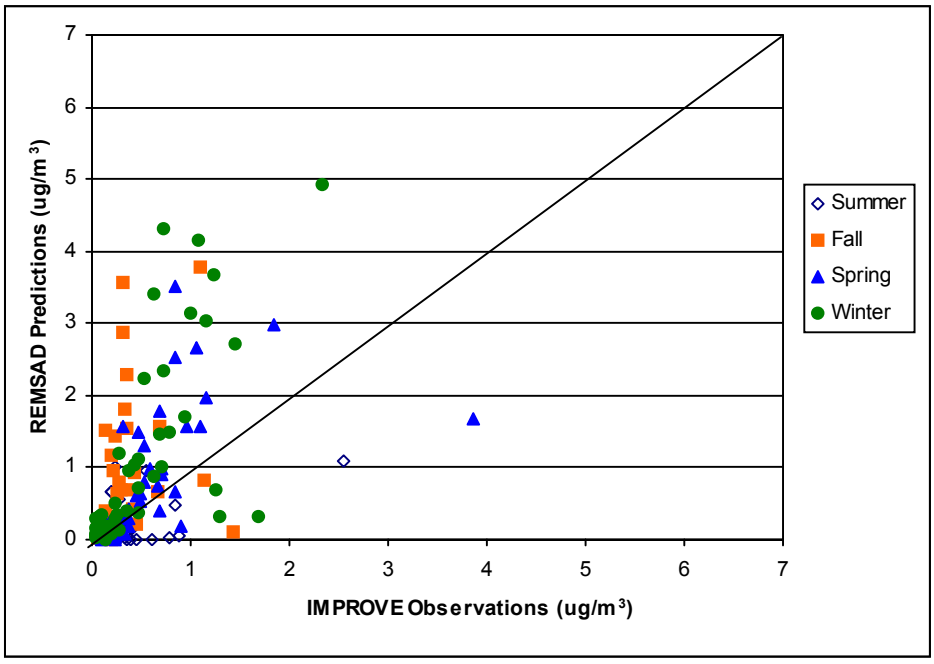

Figure IV-13. Seasonal average nitrate ion 1996 IMPROVE observations versus REMSAD predictions

a.6. PMFINE-Other (crustal) Performance

Table IV-9 lists the performance statistics for PMFINE-other or primary crustal emissions. The observations show crustal $PM_{2.5}$ to be generally higher in the West than in the East. However, REMSAD is predicting higher crustal concentrations in the East. Performance statistics show an underprediction of 19% in the west, with an overprediction nationally of ~33%. The largest categories of PMFINE-other are fugitive dust sources such as paved roads, unpaved roads, construction, and animal feed lots.

There is a large uncertainty as to how emissions for such sources should be treated in grid-based air quality models since a large fraction of the emissions either deposit or are removed by vegetation within a few meters of the source. Work is underway to develop improved methods for estimating emissions from these sources for the purpose of air quality modeling.

Table IV-9. Annual mean PMFINE (crustal) performance at IMPROVE sites.

	No. of Sites	Mean REMSAD Predictions (µg/m^3)	Mean Observations (µg/m^3)	Ratio of Means (pred/obs)	Bias (µg/m^3)	Fractional Bias (%)	Error (µg/m^3)	Fractional Error (%)	Correlation Coefficient
National	57	0.86	0.64	1.33	0.22	38.8	0.80	93.9	0.003
East	16	1.64	0.53	3.08	1.10	103.8	1.36	116.1	0.002
West	41	0.56	0.69	0.81	-0.13	13.5	0.58	85.3	0.00

Figures IV-14 and IV-15 show the annual and seasonal average concentration scatterplots for PMFINE-other.

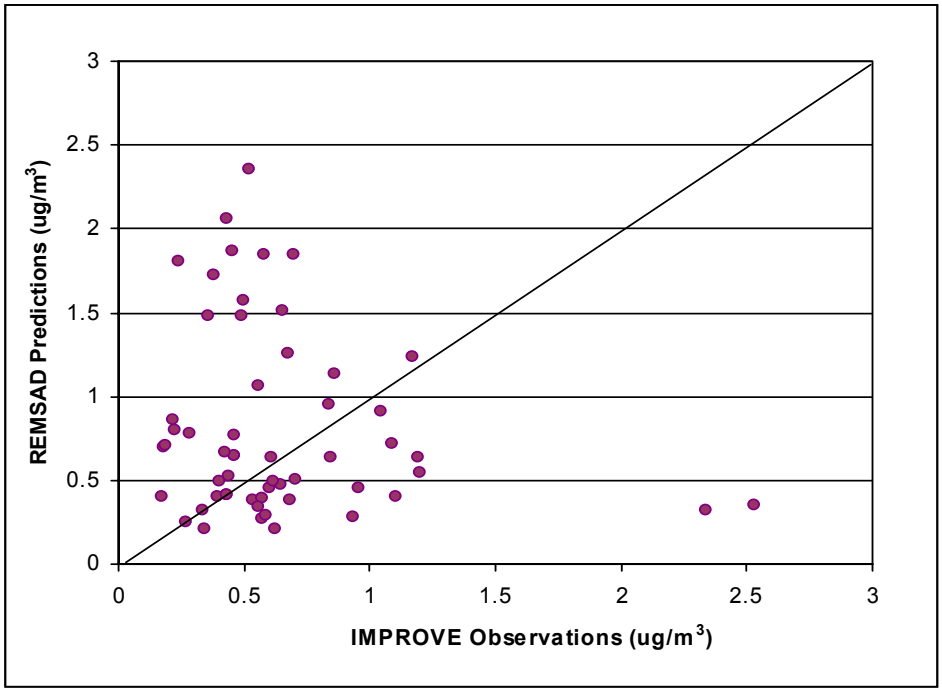

Figure IV-14. Annual average PMFINE (crustal) 1996 IMPROVE observations versus REMSAD predictions

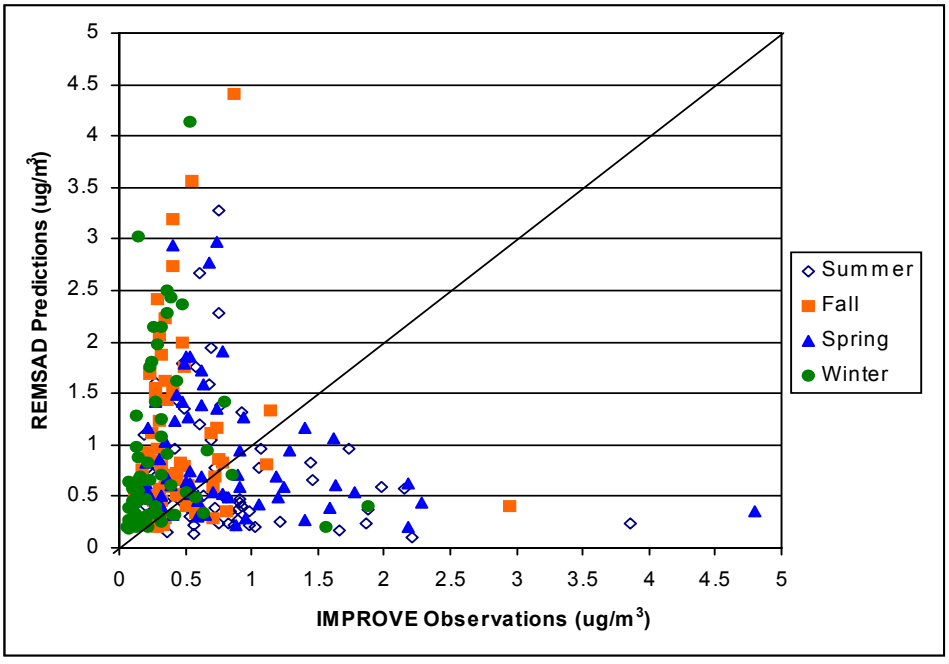

Figure IV-15. Seasonal average PMFINE (crustal) 1996 IMPROVE observations versus REMSAD predictions

b. NADP Wet Deposition Performance

Figures IV-16; 17; and 18 show the annual 1996 NADP observations versus REMSAD predictions for ammonium, nitrate, and sulfate wet deposition respectively. The scatterplots and linear regressions show some scatter (e.g. underprediction bias for nitrate and especially sulfate wet deposition), but good agreement, with strong correlations (NH_4: $R^2 = 0.65$; NO_3: $R^2 = 0.78$; SO_4: $R^2 = 0.78$).

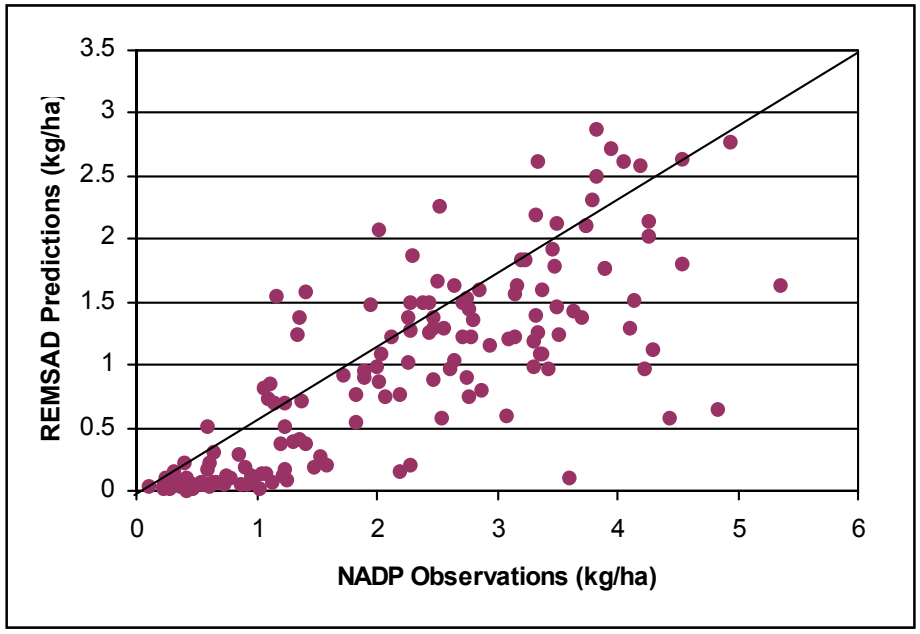

Figure IV-16. Annual total ammonium (NH_4) wet deposition 1996 NADP observations versus REMSAD predictions.

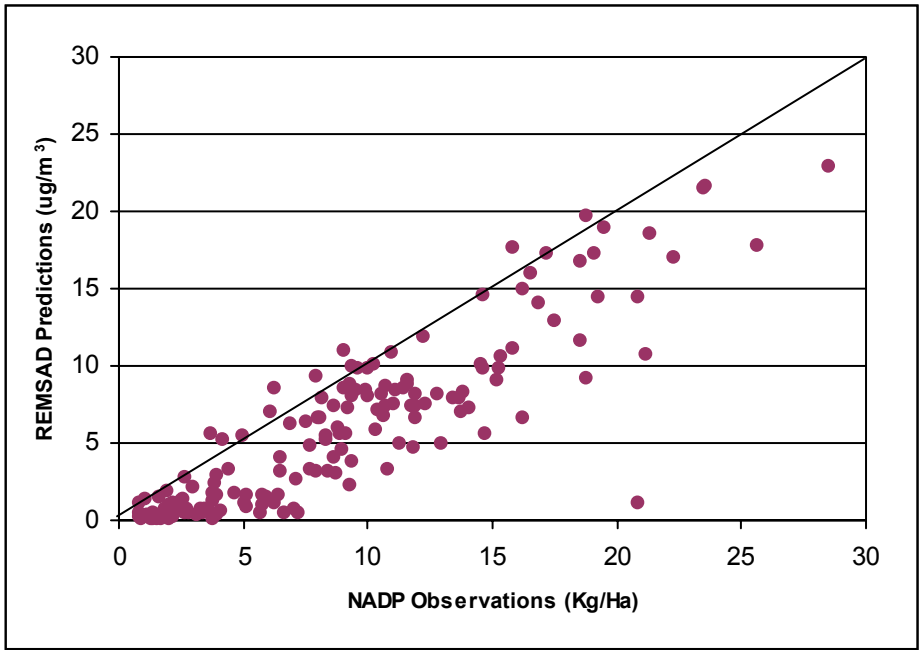

Figure IV-17. Annual total nitrate (NO_3) wet deposition 1996 NADP observations versus REMSAD predictions

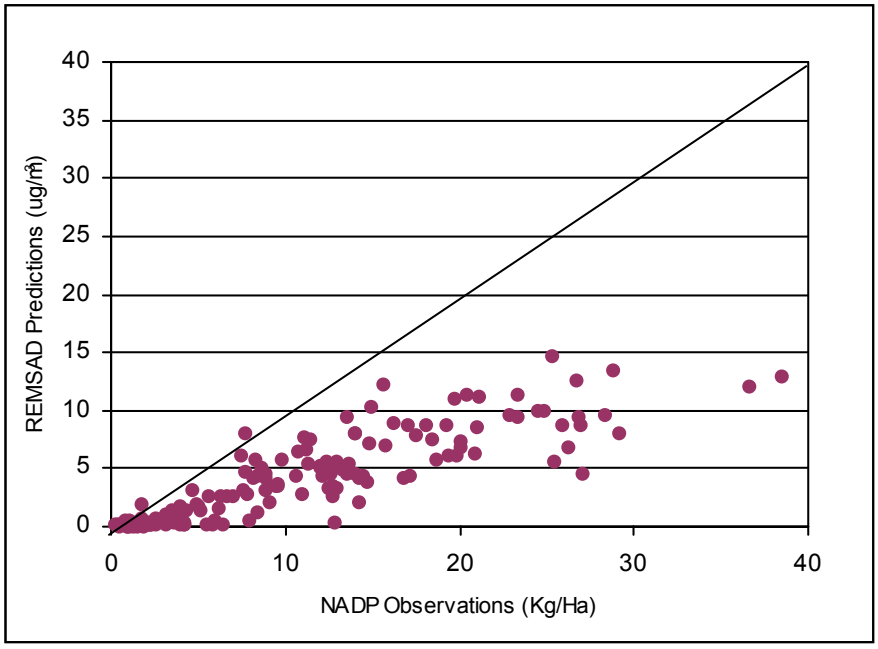

Figure IV-18. Annual total sulfate (SO_4) wet deposition 1996 NADP observations versus REMSAD predictions.

c. Wet Mercury Deposition

The Mercury Deposition Network (MDN) was in its first year of operation in 1996 with a limited number of sites[10]. Therefore, there is not enough data available to adequately judge model performance. At the few sites where there was ambient data, REMSAD predicted wet mercury deposition is underestimated compared to the observed values (mercury deposition performance is notably poorer than the other deposited species). It should be noted that REMSAD generally predicts higher levels of dry deposition of mercury compared to wet deposition. But there are no existing measurements of dry deposition to compare to the model results.

There is a great deal of uncertainty in the modeling of mercury deposition. Mercury chemistry is not fully understood. There is also uncertainty associated with the global background of mercury. Estimates of background mercury in terms of the boundary conditions assumed in the model can be very important to predicting mercury and mercury deposition. Certain forms of mercury are long lived and can be transported around the globe. In view of the uncertainty in global transport, different models and model applications have used boundary conditions for mercury that vary by as much as a factor of 5 at the surface and aloft. Additional research is needed to be able to develop representative boundary conditions. Since temporally varying boundary conditions at high altitudes may be important, it may be necessary to use results of a global mercury model to develop boundary conditions for continental scale air quality models such as REMSAD.

[10] There were 8 sites with complete annual wet deposition data.

d. CASTNet Performance

Figures IV-19 and 20 show the seasonal 1996 CASTNet observations versus REMSAD predictions for total sulfate and total nitrate, respectively. The scatterplot and linear regression of sulfate showed good agreement, with strong correlations among all seasons (summer: R^2 = 0.80; fall: R^2 = 0.92; spring: R^2 = 0.81; winter: R^2 = 0.78). The performance of sulfate at the CASTNet sites looks better than at the IMPROVE sites. The CASTNet sites measure data on a weekly average basis as opposed to the IMPROVE twice weekly sampling schedule. There are also more CASTNet sites in the high sulfate region of the East (e.g. the Ohio Valley). The CASTNet long term averaging of data seems particularly well suited for comparisons to seasonal average modeled concentrations.

The scatterplot and linear regression of total nitrate showed modest agreement, with weaker correlations within each season (summer: R^2 = 0.48; fall: R^2 = 0.67; spring: R^2 = 0.74; winter: R^2 = 0.51). There is an indication of an overprediction bias. This is not surprising given the overprediction bias of modeled particulate nitrate. The overprediction of total nitrate indicates that nitric acid concentrations may be overpredicted. This may be one of the reasons for the general overprediction of particulate nitrate. Model developers are continuing to examine the nitric acid production and destruction pathways. There are continuing improvements being made to the daytime and nighttime nitric acid formation reactions. Dry deposition of nitric acid is also being studied as a possible cause of overprediction.

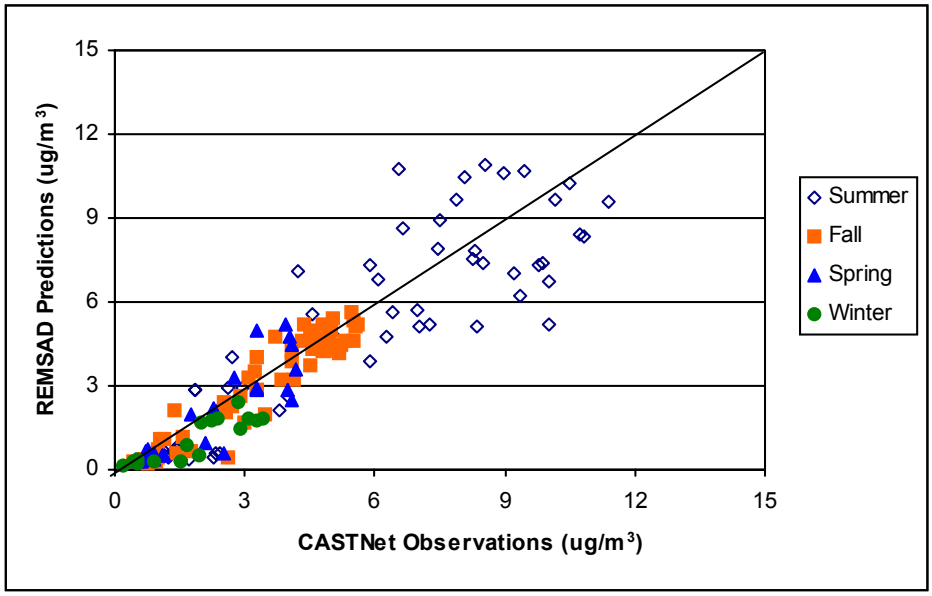

Figure IV-19. Seasonal average sulfate (SO_4) 1996 CASTNet observations versus REMSAD predictions.

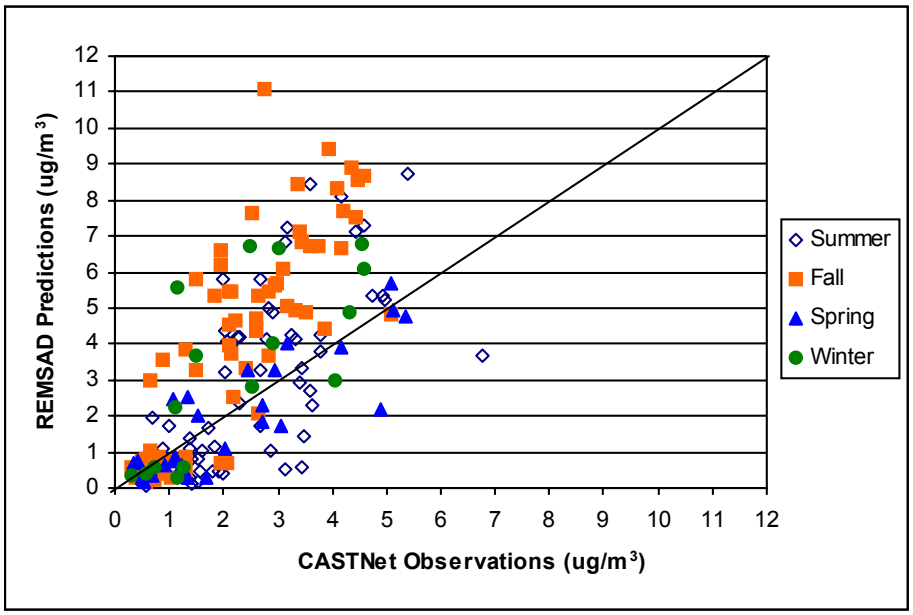

Figure IV-20. Seasonal average total nitrate ($NO_3 + HNO_3$) 1996 CASTNet observations versus REMSAD predictions.

e. Visibility performance

For the purpose of model performance evaluation, visibility was calculated in a manner similar to recommendations for the Regional Haze rule. For the Regional Haze rule, states must look at the change in visibility on the 20% best days and the 20% worst days (in units of deciviews) at each Class I area. A certain improvement in visibility on the 20% worst days is needed in the future at each Class I area. Visibility on the 20% best days cannot degrade in the future.

EPA has released a draft version of guidance that details the calculation of base period visibility (EPA, 2001a). The 20% best and worst days for the "base period" are to be calculated from the 2000-2004 IMPROVE data at each Class I area. The daily average extinction coefficient (b_{ext}) values are calculated using the following formula:

$$b_{ext} = 10.0 + [3.0 * f(RH) * (1.375 * sulfate) + 3.0 * f(RH) * (1.29 * nitrate) + 4.0 * (organic\ aerosols) + 10.0 * (elemental\ carbon) + 1.0 * (crustal) + 0.6 * (coarse\ PM)]$$

B_{ext} is in units of inverse megameters (Mm^{-1}). The 10.0 initial value accounts for atmospheric background (i.e., Rayleigh) scattering. F(RH) refers to the relative humidity correction function as defined by IMPROVE (2000). The relative humidity correction factor was derived from historical climatological meteorological data. There is a published f(rh) value for each month of the year for each Class I area (SAIC, 2001). The climatological f(rh) values will be used to calculate bext for the Regional Haze rule.

The formula to calculate b_{ext} from REMSAD output species is as follows:

b_{ext} = 10.0 + [3.0 * f(RH) * (1.375 * (GSO4 + ASO4)) + 3.0 * f(RH) * (1.29 * PNO3)+
4.0 * (TOA) + 10.0 * PEC + 1.0 * (PMFINE) + 0.6 * (PMCOARS)]

The daily average bext values are converted to deciview values using the following formula:

$$dv = 10.0 * \ln\left[\frac{(b_{ext})}{10.0\ Mm^{-1}}\right]$$

The 20% best and worst days are identified based on the daily average **observed** deciview values at each Class I areas. For the purpose of this model performance evaluation, we have calculated the 20% best and worst days from 1996 (the meteorological year we are using) at each IMPROVE site with complete data. The following scatter plots show the observed vs. predicted b_{ext} values at the IMPROVE sites on the 20% best and worst days.

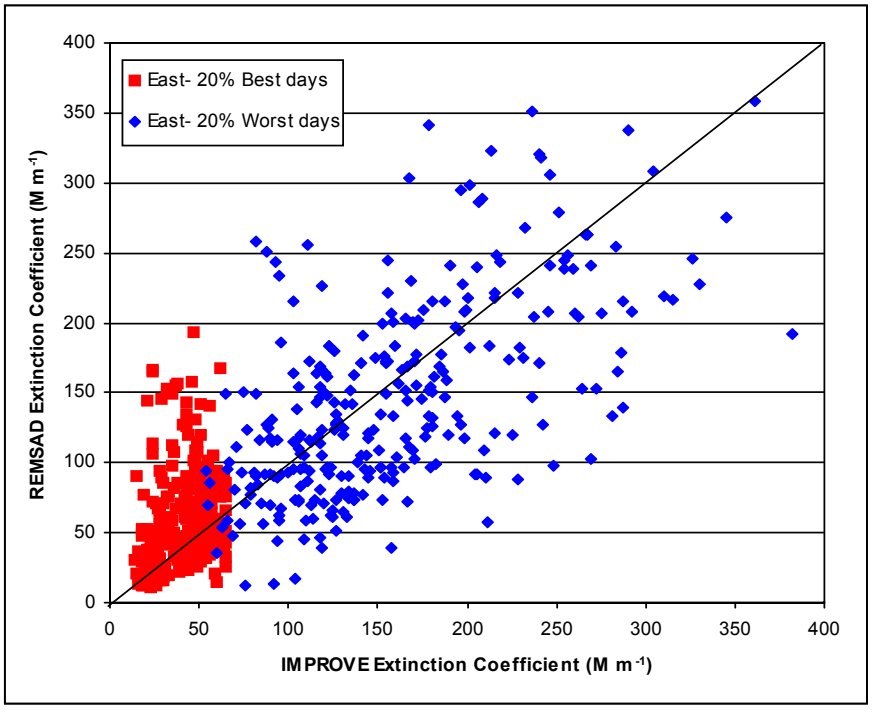

Figure IV-21. IMPROVE observed versus REMSAD predicted light extinction coefficient values on the 20% best and worst days in the East.

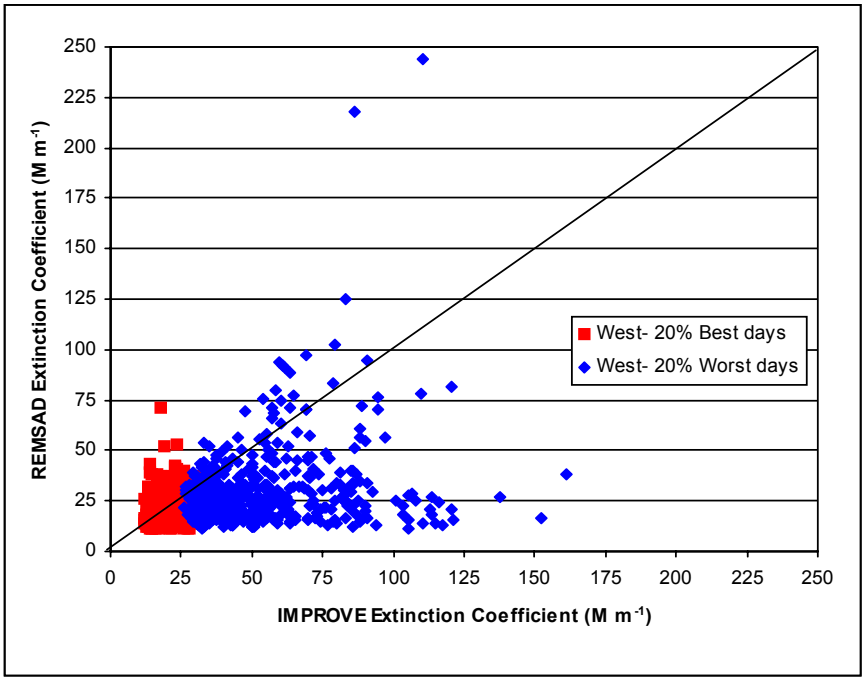

Figure IV-22. IMPROVE observed versus REMSAD predicted light extinction coefficient values on the 20% best and worst days in the West.

REMSAD was generally able to predict the highest b_{ext} values on the observed worst days in the East. The 20% worst days in the East show little bias, but a large amount of scatter. The 20% best days in the East are generally overpredicted. The 20% worst days in the West are underpredicted. REMSAD rarely predicted high b_{ext} values in the West. The model predictions on the 20% best and worst days are similar.

3. Summary of Model Performance

The purpose of this model performance evaluation was to evaluate the capabilities of the REMSAD modeling system in reproducing annual average concentrations and deposition at all IMPROVE, CASTNet, and NADP sites in the contiguous U.S. for fine particulate mass, its associated speciated components, visibility, and wet deposition. When considering annual average statistics (e.g., predicted versus observed), which are computed and aggregated over all sites and all days, REMSAD underpredicted fine particulate mass ($PM_{2.5}$), by 18%. $PM_{2.5}$ in the Eastern U.S. was underpredicted by 2%, while $PM_{2.5}$ in the West was underpredicted by 33%. All $PM_{2.5}$ component species were underpredicted in the west. In the East, nitrate and crustal material are overestimated. Elemental carbon shows neither over or underprediction in the east with a bias near 0%. Eastern sulfate is slightly underpredicted with a bias of 12%. Organic aerosols show little or no bias in the East and West.

The comparisons to the CASTNet data show generally good model performance for particulate sulfate. Comparison of total nitrate indicate an overestimate, possible due to overpredictions of nitric acid in the model.

Performance at the NADP sites for wet deposition of ammonium, sulfate, and nitrate were reasonably good. There is a an underprediction bias of nitrate, and especially sulfate wet deposition. The model predictions of total mercury wet deposition at the MDN sites were also underpredicted.

Given the state of the science relative to PM modeling, it is inappropriate to judge PM model performance using criteria derived for other pollutants, like ozone. Still, the performance of the Clear Skies PM modeling is very encouraging, especially considering that the results may be limited by our current knowledge of PM science and chemistry, by the emissions inventories for primary PM and secondary PM precursor pollutants, by the relatively sparse ambient data available for comparisons to model output, and by uncertainties in monitoring techniques. The model performance for sulfate is quite reasonable, which is key to the Clear Skies analysis due to the importance of SO_2 emissions reductions in the Clear Skies control program.

It is important to note that there are a number of factors to be considered when interpreting the results of this performance analysis. First, simulating the formation and fate of particles, especially secondary organic aerosols and nitrates are part of an evolving science. In this regard, the science in air quality models is continually being updated as new research results become available. Also, there are a number of issues associated with the emissions and meteorological inputs, as well as ambient air quality measurements and how these should be paired to model predictions that are currently under investigation by EPA and others. The process of building consensus within the scientific community on ways for doing PM model performance evaluations has not yet progressed to the point of having a defined set of common approaches or criteria for judging model performance. Unlike ozone, there is a limited database of past performance statistics against which to measure the performance of the Clear Skies PM modeling. Thus, the approach used for this analysis may be modified or expanded in future evaluation analyses.

E. Projected Future $PM_{2.5}$ Design Values

1) East

The REMSAD simulations were performed for Base Cases in 1996, 2001, 2010, and 2020 considering growth and expected emissions controls that will affect future air quality. The effects of the Clear Skies Act emissions reductions (i.e., Control Cases) were modeled for the two future years (2010 and 2020). As a means of assessing the future levels of air quality with regard to the $PM_{2.5}$ NAAQS, future-year estimates of $PM_{2.5}$ design values were calculated using relative reduction factors (RRFs) applied to 1999-2001 $PM_{2.5}$ design values (EPA, 2003b). The procedures for determining the RRFs are similar to those in EPA's draft guidance for modeling the $PM_{2.5}$ standard (EPA, 1999a). The guidance recommends that model predictions be used in a relative sense to estimate changes expected to occur in each major $PM_{2.5}$ species. These species are sulfate, nitrate, organic carbon, elemental carbon, crustal and un-attributed mass which is defined as the difference between measured $PM_{2.5}$ and the sum of the other five components. The procedure for calculating future year $PM_{2.5}$ design values is called the "Speciated Modeled Attainment Test (SMAT)". EPA used this procedure to estimate the ambient impact of the Clear Skies Act emissions controls.

The guidance describes a sequence of key steps that are recommended in processing the data. The following is a brief summary of those steps:

1. Derive current quarterly mean concentrations (averaged over three years) for each of the six major components of $PM_{2.5}$. This is done by multiplying the monitored quarterly mean concentration of Federal Reference Method (FRM) derived $PM_{2.5}$ by the monitored fractional composition of $PM_{2.5}$ species (at speciation monitor sites) for each quarter in three consecutive years. (e.g., 20% sulfate x 15 $\mu g/m^3$ $PM_{2.5}$ = 3 $\mu g/m^3$ sulfate).

2. For each quarter, apply an air quality model to estimate current and future concentrations for each of the six components of $PM_{2.5}$. Take the ratio of future to current predictions for each component. The result is a component-specific *relative reduction factor* (RRF). (e.g., given model predicted sulfate for base is 10 $\mu g/m^3$ and future is 8 $\mu g/m^3$ then RRF for sulfate is 0.8).

3. For each quarter, multiply the current quarterly mean component concentration (step 1) times the component-specific RRF obtained in step 2. This leads to an estimated future quarterly mean concentration for each component. (e.g., 3 $\mu g/m^3$ sulfate x 0.8 = future sulfate of 2.4 $\mu g/m^3$).

4. Average the four quarterly mean future concentrations to get an estimated future annual mean concentration for each component. Sum the annual mean concentrations of the six components to obtain an estimated future annual concentration for $PM_{2.5}$.

EPA will use the Federal Reference Monitor (FRM) data for nonattainment designations. Therefore it is critical that FRM data is used in the speciated modeled attainment test described above. As can be seen from the list of steps, the modeled attainment test is critically dependent on the availability of species component mass at FRM sites. There is currently a limited

database of urban speciation data from the Speciation Trends Network (STN)[11]. Therefore, a spatial interpolation methodology was developed to estimate component species mass at the FRM locations. Additional ambient data handling procedures were also developed. Full documentation of the procedures and assumptions used in the future year design value calculations is contained in Appendix E.

The SMAT procedure was performed using the base year 2001 scenario and each of the future-year scenarios. $PM_{2.5}$ component species RRFs were calculated on a site-by-site basis. The future-year design value projections were then calculated by county, based on the highest resultant design values for a site within that county. The current and future base and control annual average $PM_{2.5}$ design values are provided in Appendix F. County populations are also included in this appendix.

2) West

Western US $PM_{2.5}$ concentrations were modeled as part of the Clear Skies analysis. But due to the lack of $PM_{2.5}$ species spatial fields, the SMAT technique was not applied. Instead, the relative reduction factors were calculated based on the predicted percentage change in total $PM_{2.5}$. This was the method of calculating future year $PM_{2.5}$ values used in past analyses. The future year design values for the West were calculated using the 1999-2001 ambient design values, the 2001 base year scenario and the 2010 and 2020 future year scenarios.

There are no western $PM_{2.5}$ nonattainment counties outside of California (except for Lincoln county, MT)[12]. As stated earlier, the projected NO_X emissions reductions in California from Clear Skies is very small (~1300 tons/year). There are also no projected Clear Skies SO_2 emissions reductions in California. Therefore, Clear Skies is expected to have no impact on $PM_{2.5}$ attainment status in California, and hence the West. Other Federal and state emissions control programs contained in the 2010 and 2020 base cases are predicted to bring several California counties into attainment for the $PM_{2.5}$ standard. The current and future base and control annual average $PM_{2.5}$ design values are provided in Appendix F.

[11] Even when the STN is completely deployed, approximately 80% of the FRM monitoring sites will not have a co-located speciation monitor.

[12] Lincoln county, Montana (Libby) is known to have a local direct $PM_{2.5}$ problem associated with its location in a river valley. It is not thought to be heavily influenced by utility emissions.

F. $PM_{2.5}$ Nonattainment Summary

As shown in Table III-10, the REMSAD modeling projects that 80 counties across the country with a population of 53.6 million people will have design values greater than the annual $PM_{2.5}$ NAAQS in 2010 without Clear Skies controls. By 2020 that number is expected to fall to 53 counties with a population of 45.7 million people as a result of projected emissions reductions from existing control programs.

Clear Skies emissions reductions are predicted to bring 42 counties with a population of 13.7 million people into attainment for the $PM_{2.5}$ standard in 2010. The reduction of 42 counties leaves 38 counties with a population of 39.9 million people nonattainment for the $PM_{2.5}$ standard in 2010 after Clear Skies controls. In 2020 Clear Skies is expected to bring 35 counties into with a population of 12.4 million people into attainment. That leaves 18 counties with a population of 33.2 million people nonattainment for the $PM_{2.5}$ standard in 2020 after Clear Skies controls. Appendix G contains maps of the base year and projected year $PM_{2.5}$ nonattainment counties.

Table III-10. Lists of counties projected to violate the Annual $PM_{2.5}$ NAAQS in 2010 and 2020 for the Base Case and Clear Skies Control Case

2010 Base	2010 Control	2020 Base	2020 Control
Alabama, Houston	Alabama, Talladega	Alabama, Montgomery	Alabama, Jefferson
Alabama,Shelby	Alabama, Russell	Alabama, Talladega	California, San Diego
Alabama, DeKalb	Alabama, Morgan	Alabama, Russell	California, Merced
Alabama, Montgomery	Alabama, Jefferson	Alabama, Morgan	California, Stanislaus
Alabama, Talladega	California, San Diego	Alabama, Jefferson	California, Orange
Alabama, Russell	California, Merced	California, San Diego	California, Kern
Alabama, Morgan	California, Stanislaus	California, Merced	California, Fresno
Alabama, Jefferson	California, Orange	California, Stanislaus	California, Tulare
California, San Diego	California, Kern	California, Orange	California, San Bernardino
California, Merced	California, Fresno	California, Kern	California, Los Angeles
California, Stanislaus	California, Tulare	California, Fresno	California, Riverside
California, Orange	California, San Bernardino	California, Tulare	Georgia, DeKalb
California, Kern	California, Los Angeles	California, San Bernardino	Georgia, Fulton
California, Fresno	California, Riverside	California, Los Angeles	Illinois, Cook
California, Tulare	Georgia, Bibb	California, Riverside	Michigan, Wayne
California, San Bernardino	Georgia, Wilkinson	Georgia, Chatham	Ohio, Jefferson
California, Los Angeles	Georgia, Muscogee	Georgia, Dougherty	Ohio, Cuyahoga

California, Riverside	Georgia, Floyd	Georgia, Richmond	Pennsylvania, Allegheny
Connecticut, New Haven	Georgia, Cobb	Georgia, Bibb	
D.C.,District of Columbia	Georgia, Clarke	Georgia, Wilkinson	
Delaware, New Castle	Georgia, Clayton	Georgia, Muscogee	
Georgia, Washington	Georgia, DeKalb	Georgia, Floyd	
Georgia, Chatham	Georgia, Fulton	Georgia, Cobb	
Georgia, Dougherty	Illinois, Madison	Georgia, Clarke	
Georgia, Paulding	Illinois, St. Clair	Georgia, Clayton	
Georgia, Richmond	Illinois, Cook	Georgia, DeKalb	
Georgia, Hall	Michigan, Wayne	Georgia, Fulton	
Georgia, Bibb	Montana, Lincoln	Illinois, Madison	
Georgia, Wilkinson	New York, New York	Illinois, St. Clair	
Georgia, Muscogee	Ohio, Franklin	Illinois, Cook	
Georgia, Floyd	Ohio, Stark	Indiana, Marion	
Georgia, Cobb	Ohio, Jefferson	Indiana, Clark	
Georgia, Clarke	Ohio, Hamilton	Maryland, Baltimore city	
Georgia, Clayton	Ohio, Scioto	Michigan, Wayne	
Georgia, DeKalb	Ohio, Cuyahoga	New York, New York	
Georgia, Fulton	Pennsylvania, Allegheny	Ohio, Summit	
Illinois, Will	Tennessee, Hamilton	Ohio, Butler	
Illinois, Madison	Tennessee, Knox	Ohio, Montgomery	
Illinois, St. Clair		Ohio, Franklin	
Illinois, Cook		Ohio, Stark	
Indiana, Lake		Ohio, Jefferson	
Indiana, Marion		Ohio, Hamilton	
Indiana, Clark		Ohio, Scioto	
Kentucky, Fayette		Ohio, Cuyahoga	
Kentucky, Jefferson		Pennsylvania, Philadelphia	
Maryland, Baltimore city		Pennsylvania, Allegheny	
Michigan, Wayne		Tennessee, Hamilton	
Mississippi, Jones		Tennessee, Knox	
Missouri, St. Louis city		West Virginia, Hancock	

Montana, Lincoln		West Virginia, Brooke	
New York, New York		West Virginia, Wood	
North Carolina, Mecklenburg		West Virginia, Cabell	
North Carolina, Catawba		West Virginia, Kanawha	
North Carolina, Davidson			
Ohio, Trumbull			
Ohio, Mahoning			
Ohio, Summit			
Ohio, Butler			
Ohio, Montgomery			
Ohio, Franklin			
Ohio, Stark			
Ohio, Jefferson			
Ohio, Hamilton			
Ohio, Sioto			
Ohio, Cuyahoga			
Pennsylvania, Philadelphia			
Pennsylvania, Lancaster			
Pennsylvania, Allegheny			
South Carolina, Greenville			
Tennessee, Sullivan			
Tennessee, Roane			
Tennessee, Davidson			
Tennessee, Hamilton			
Tennessee, Knox			
West Virginia, Marshall			
West Virginia, Hancock			
West Virginia, Brooke			
West Virginia, Wood			
West Virginia, Cabell			
West Virginia, Kanawha			
80 Counties	**38 Counties**	**53 Counties**	**18 Counties**

G. Projected Visibility

As described previously, visibility was calculated for the 20% best and worst days from 1996 at each IMPROVE site with complete data. The future year projected visibility was also calculated for each Clear Skies scenario in 2010 and 2020 using a methodology similar to SMAT. The draft modeling guidance recommends the calculation of future year changes in visibility in a similar manner to the calculation of changes in $PM_{2.5}$. The extinction coefficient and deciview values are made up of individual component species (sulfate, nitrate, organics, etc). The predicted change in visibility (on the 20% best and worst days) is calculated as the summed percent change in the extinction coefficient for each of the PM species (on a daily basis). The daily average extinction coefficients are converted to deciviews and then averaged (best and worst days separately). In this way, we can calculate an average change in deciviews from the base case to a future case at each IMPROVE site.

Appendix H contains an example calculation of the predicted improvement in visibility on the 20% worst days at an IMPROVE site as well as the predicted reductions in visibility at Class I areas on the 20% best visibility days and the 20% worst visibility days. There is a separate table for the 20% best days and 20% worst days. The calculated reductions in deciviews is based on the model predicted changes in PM species between the 2001 proxy base case and the 2010 and/or 2020 model runs. The calculated reductions in deciviews are from a base line of 1996 ambient data. The 1996 ambient data was only used as a starting point to calculate the deciview reductions.[13]

As an example, the expected improvement in visibility at the Great Smoky Mountain National Park (GRSM) on the 20% worst visibility days in 2010 without Clear Skies is 1.38 deciviews. The expected improvement with Clear Skies controls (in addition to all other expected controls) is 3.37 deciviews. The improvement in visibility due only to Clear Skies controls is 1.99 deciviews. The expected improvement in visibility in 2020 is even larger. The visibility improvement without Clear Skies is 2.28 deciviews. The improvement with Clear Skies is 5.56 deciviews, resulting in an improvement due only to Clear Skies controls of 3.29 deciviews.

The Clear Skies modeling predicts smaller improvements in visibility on the 20% best days. But there are no cases in which visibility deteriorated due to Clear Skies or any other controls. There are some Class I areas in the West which do not show any improvement in visibility due to Clear Skies. This is not surprising due to the very small emissions reductions in California and other Western states.

---

[13] The 1996 data was used because it is coincident with the REMSAD meteorology. The changes in visibility are representative of emissions changes from 2001 into the future (not 1996). Due to the lack of complete IMPROVE baseline ambient data and due to the fact that 1996 meteorology was used, it was difficult to replicate the Regional Haze guidance (the modeling guidance and the procedures for calculating the baseline 20% best and worst days.) The resultant values are believed to be representative of the expected improvement in visibility.

H. Model outputs for benefits calculations

A number of model outputs are provided for economic and health benefits calculations. The following model outputs were provided for each modeling scenario:

CAMx

Hourly average ozone concentration

REMSAD

Daily average PM2.5 concentrations
Daily average PM10 concentrations
Annual average visibility[14]
Annual average PM2.5 concentrations
Annual average PM10 concentrations
Annual total nitrogen deposition
Annual total sulfur deposition
Annual total mercury deposition

[14] The daily average modeled b_{ext} values are averaged to derive the annual average b_{ext}. The annual average b_{ext} were used to calculate the annual average deciviews (dv). The relative humidity correction factor f(rh) used to calculate the annual average visibility was calculated from the hourly average modeled relative humidity at each grid cell for each time period. The climatological f(rh) values at each Class I area could not be used because annual average visibility calculations are needed for each grid cell.

V. References

Environ, 2002: User's Guide: Comprehensive Air Quality Model with Extensions (CAMx), Novato, CA.

EPA, 1991: Guideline for Regulatory Application of the Urban Airshed Model, EPA-450/4-91-013, Office of Air Quality Planning and Standards, Research Triangle Park, NC.

EPA, 1999a: Draft Guidance on the Use of Models and Other Analyses in Attainment Demonstrations for the 8-Hour Ozone NAAQS, Office of Air Quality Planning and Standards, Research Triangle Park, NC.

EPA, 1999b: Technical Support Document for the Tier 2/Gasoline Sulfur Ozone Modeling Analyses, EPA420-R-99-031, Research Triangle Park, NC.

EPA, 2000a: Technical Support Document for the Heavy Duty Engine and Vehicle Standards and Highway Diesel Fuel Sulfur Control Requirements: Air Quality Modeling Analyses, EPA420-R-00-0208, Research Triangle Park, NC.

EPA, 2000b: Guidance for Demonstrating Attainment of Air Quality Goals for $PM_{2.5}$ and Regional Haze; Draft 1.1, Office of Air Quality Planning and Standards, Research Triangle Park, NC.

EPA, 2001a: Draft Guidance for Tracking Progress Under the Regional Haze Rule, Office of Air Quality Planning and Standards, Research Triangle Park, NC.

EPA, 2001b: Draft Guidance for Estimating Natural Visibility Conditions Under the Regional Haze Program, Office of Air Quality Planning and Standards, Research Triangle Park, NC.

EPA, 2002: Clean Air Status and Trends Network (CASTNet), 2001 Annual Report.

EPA, 2003a: Procedures for Developing Base Year and Future Year Mass Emissions Inventories for the Nonroad Diesel Engine Rulemaking, Office of Air Quality Planning and Standards, Research Triangle Park, NC.

EPA, 2003b: Air Quality Data Analysis 1999-2001, Technical Support Document for Regulatory Actions, Office of Air Quality Planning and Standards, Research Triangle Park, NC.

EPA, 2003c: Technical Support Document for the Nonroad Land-Based Diesel Engine Standards: Air Quality Modeling Analyses, Office of Air Quality Planning Services, Research Triangle Park, NC.

Grell, G., J. Dudhia, and D. Stauffer, 1994: A Description of the Fifth-Generation Penn State/NCAR Mesoscale Model (MM5), *NCAR/TN-398+STR*., 138 pp, National Center for Atmospheric Research, Boulder CO.

Houyoux, M.; Vukovich, J.; Brandmeyer, J. *Sparse Matrix Operator Kernal Emissions Modeling System (SMOKE) User Manual*, Version 1.1.2 Draft, MCNC-North Carolina Supercomuting Center Environmental Programs, 2000. (Updates at http://www.cmascenter.org/modelclear.html#smoke)

ICF Kaiser, 2002: User's Guide to the Regional Modeling System for Aerosols and Deposition (REMSAD) Version 7, San Rafael, CA.

IMPROVE. 2000. Spatial and Seasonal Patterns and Temporal Variability of Haze and its Constituents in the United States: Report III. Cooperative Institute for Research in the Atmosphere, ISSN: 0737-5352-47.

Griffin, R.J., D.R. Cocker III, R.C. Flagan, and J.H. Seinfeld, 1999: "Organic aerosol formation from the oxidation of biogenic hydrocarbons" *J. Geophysical Research*, Vol. 104, pp. 3555-3567.

Kim, Y.P., J.H. Seinfeld, and P. Saxena, 1993. "Atmospheric Gas-Aerosol Equilibrium I. Thermodynamic Model." *Aerosol Science and Technology*, Vol. 19, pp. 157-181.

Mansell, G., 2000: User's Instructions for the Phase 2 REMSAD Preprocessors, Environ International, Novato, CA.

NADP, 2002: National Acid Deposition Program 2002 Annual Summary.

Odum, J.R., T.P.W. Jungkamp, R.J. Griffin, R.C. Flagan, and J.H. Seinfeld, 1997: "The Atmospheric Aerosol-Forming Potential of Whole Gasoline Vapor" *Science*, Vol. 276, pp. 96-99.

Olerud, D., K. Alapaty, and N. Wheeler, 2000: Meteorological Modeling of 1996 for the United States with MM5. MCNC-Environmental Programs, Research Triangle Park, NC.

Pielke, R.A., W.R. Cotton, R.L. Walko, C.J. Tremback, W.A. Lyons, L.D. Grasso, M.E. Nicholls, M.D. Moran, D.A. Wesley, T.J. Lee, and J.H. Copeland, 1992: A Comprehensive Meteorological Modeling System - RAMS, *Meteor. Atmos. Phys*., Vol. 49, pp. 69-91.

Saxena, P., A.B. Hudischewskyj, C. Seigneur, and J.H. Seinfeld, 1986: "A Comparative Study of Equilibrium Approaches to the Chemical Characterization of Secondary Aerosols." *Atmospheric Environment*, Vol. 20, pp. 1471-1483.

Seigneur, C., G. Hidy, I. Tombach, J. Vimont, P. Amar, 1999: "Scientific Peer-Review of the Regulatory Modeling System for Aerosols and Deposition (REMSAD)." The KEVRIC Company, Inc., Durham, NC.

Sistla, Gopal, 1999: Personal communication.

SAIC, 2001: "Interpolating Relative Humidity Weighting Factors to Calculate Visibility Impairment and the Effects of Improve Monitor Outliers" EPA Contract No. 68-D-98-113. http://vista.cira.colostate.edu/improve/Publications/GuidanceDocs/DraftReportSept20.pdf

Systems Applications International, 1996: User's Guide to the Variable-Grid Urban Airshed Model (UAM-V), SYSAPP-96-95/27r, San Rafael CA.

Wesley, M.L., 1989: "Parameterization of Surface Resistances to Gaseous Dry Deposition in Regional-Scale Numerical Models" Atmospheric Environment, Vol. 23, No 6, pp. 1293-1304.

Whitten, Gary Z., 1999: Computer Efficient Photochemistry for Simultaneous Modeling of Smog and Secondary Particulate Precursors, Systems Application International, San Rafael, CA.